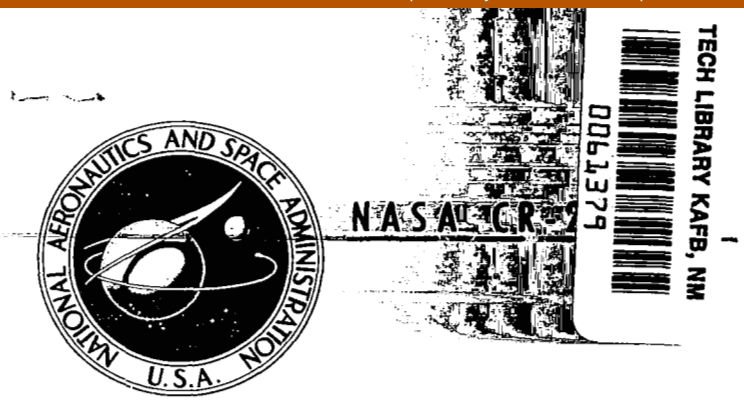


NASA CONTRACTOR REPORT

NASA CR-2782



# CHARACTERISTICS OF THE MOTIONS, TURBULENCE INTENSITY, DIFFUSIVITY, FLUX OF MOMENTUM AND SENSIBLE HEAT IN THE UPPER ATMOSPHERE

*S. K. Kao and N. J. Lordi*

*Prepared by*
UNIVERSITY OF UTAH
Salt Lake City, Utah 85112
*for Wallops Flight Center*

NATIONAL AERONAUTICS AND SPACE ADMINISTRATION • WASHINGTON, D. C. • FEBRUARY 1977

| 1. Report No. | 2. Government Accession No. | 3. Recipient's Catalog No. |
|---|---|---|
| NASA CR-2782 | | |

| 4. Title and Subtitle | 5. Report Date |
|---|---|
| CHARACTERISTICS OF THE MOTIONS, TURBULENCE INTENSITY, DIFFUSIVITY, FLUX OF MOMENTUM AND SENSIBLE HEAT IN THE UPPER ATMOSPHERE | February 1977 |
| | 6. Performing Organization Code |

| 7. Author(s) | 8. Performing Organization Report No. |
|---|---|
| S. K. Kao and N. J. Lordi | |
| | 10. Work Unit No. |

| 9. Performing Organization Name and Address | 11. Contract or Grant No. |
|---|---|
| Department of Meteorology<br>University of Utah<br>Salt Lake City, UT 85112 | NAS6-2498 |
| | 13. Type of Report and Period Covered |
| 12. Sponsoring Agency Name and Address | Contractor Report |
| National Aeronautics and Space Administration<br>Wallops Flight Center<br>Wallops Island, VA 23337 | 14. Sponsoring Agency Code |

15. Supplementary Notes

16. Abstract

Analyses of the meteorological rocket data obtained from an experiemnt conducted at 3-hour intervals on 19-20 March 1974 at 8 western meridional rocket stations indicate that:

1. Large variations in the meridional wind contribute substantially to overall turbulence in the tropical stratosphere.

2. The solar semidiurnal component of wind oscillations in the tropics was observed to be much higher than predicted by theory, often exceeding the magnitude of the diurnal amplitude throughout the stratosphere.

3. The observed value of the solar diurnal amplitude in the stratosphere was in line with theoretical prediction.

4. The solar terdiurnal amplitudes for temperature, meridional and zonal winds were non-negligible and must be considered in any harmonic analysis.

5. Phase angle variation with height was rapid for all harmonics; however, there was general agreement between predicted and observed phase angles.

6. Because of large changes in the mean winds in the mesosphere with season, harmonic determinations are difficult. There appear to be large zonal wind changes even within the same season as mentioned previously.

7. Turbulence diffusivity in the upper stratosphere is greater near the equator than in the mid-latitudes.

| 17. Key Words (Suggested by Author(s)) | 18. Distribution Statement |
|---|---|
| Meteorology, Diurnal Variations, Transport Coefficients, Heat Transfer, Turbulence, Meteorological Rockets | Unclassified - unlimited<br>STAR Category 47 |

| 19. Security Classif. (of this report) | 20. Security Classif. (of this page) | 21. No. of Pages | 22. Price* |
|---|---|---|---|
| Unclassified | Unclassified | 57 | $4.50 |

* For sale by the National Technical Information Service, Springfield, Virginia 22161

# CHARACTERISTICS OF THE MOTIONS, TURBULENCE INTENSITY, DIFFUSIVITY, FLUX OF MOMENTUM AND SENSIBLE HEAT IN THE UPPER ATMOSPHERE

by

S. K. KAO and N. J. Lordi
University of Utah

## SUMMARY

Analyses of the meteorological rocket data obtained from an experiment conducted at 3-hour intervals on 19-20 March 1974 at 8 western meridional rocket stations indicate that:

1) Large variations in the meridional wind contribute substantially to overall turbulence in the tropical stratosphere.

2) The solar semidiurnal component of wind oscillations in the tropics was observed to be much higher than predicted by theory, often exceeding the magnitude of the diurnal amplitude throughout the stratosphere.

3) The observed value of the solar diurnal amplitude in the stratosphere was in line with theoretical predictions.

4) The solar terdiurnal amplitudes for temperature, meridional and zonal winds were non-negligible and must be considered in any harmonic analysis.

5) Phase angle variation with height was rapid for all harmonics; however, there was general agreement between predicted and observed phase angles.

6) Because of large changes in the mean winds in the mesosphere with season, harmonic determinations are difficult. There appear to be large zonal wind changes even within the same season as mentioned previously.

7) Turbulence diffusivity in the upper stratosphere is greater near the equator than in the mid-latitudes.

## INTRODUCTION

The region of the atmosphere between 30 and 60 km has always been data sparse, and hence, actual determinations of solar and lunar tidal characteristics in this region have been few and far between. Beyers, Miers and Reed (1966), analyzing 16 rocket soundings over 51 hours at White Sands Missile Range between 30 June and 2 July 1965, found strong diurnal wind variations above 40 km. Reed, McKenzie and Vyverberg (1966) used the routine soundings at White Sands and Cape Kennedy during the summer to obtain diurnal variations of the meridional wind. They found an amplitude of less than 1 m/s below 37 km with a rapid rise to about 8 m/s near 50 km and a decrease from this value at higher altitudes. Combining soundings from stations at proximate latitudes, Reed, Oard and Sieminski (1969) fitted diurnal and semidiurnal harmonics to irregularly spaced data by the least squares method. A shortcoming of this method is that it presupposes that variations are due only to diurnal and semidiurnal oscillations. The method is obviously less meaningful if this assumption breaks down.

On 19-20 March 1974 an experiment, conducted as part of the Western Meridional Rocket Network, was completed in which rocket soundings were taken at each of 8 stations with launchings scheduled at 3-hour intervals at each station over a

period of 24 hours. The stations participating in the experiment were: Natal, Brazil (5.9°S), Kourou, French Guiana (5.1°N), Wallops Island, Virginia (37.8°N), Fort Sherman, Panama Canal Zone (9.3°N), Antigua, British West Indies (17.2°N), Ascension Island (8.0°S), Fort Churchill, Canada (57.1°N) and Mar Chiquita, Argentina (39.°S). Due to technical difficulties, some of the scheduled launches did not go off, and hence only one station (Kourou, French Guiana) has a complete set of data (equally spaced in time).

One purpose of the present study is to harmonically analyze the above mentioned rocket data to obtain amplitudes and phase angles of the various solar harmonic contributions. Where necessary, missing data were filled in using cubic spline interpolation. Another objective of our study is the analysis of turbulence intensity, eddy diffusivity, and meridional turbulent transports of heat and zonal momentum.

## DATA REDUCTION

The winds used in this study were obtained on 19-20 March 1974 during an experiment conducted as part of the Western Meridional Rocket Network. It was hoped that rocket soundings would be taken at 3-hour intervals at each of 8 stations - Natal, Brazil (5.9°S), Kourou, French Guiana (5.1°N), Wallops Island, Virginia (37.8°N), Fort Sherman, Panama Canal Zone (9.3°N), Antigua, British West Indies (17.2°N), Ascension Island (8.0°S), Fort Churchill, Canada (57.1°N) and Mar Chiquita, Argentina (39.°S). Due to technical difficulties at launch sites the above objective was only achieved at Kourou, French Guiana. Thus, data were missing for certain times; and since to perform a harmonic analysis equally spaced data are required, interpolation of winds and temperatures at missing times was necessary. The interpolation scheme used was the natural cubic spline, which will be described in the next section.

The flight system used for data gathering was either the Loki datasonde or Super Loki datasonde. A 10 mil bead loop mount was used as a temperature sensor, and either a

7-ft or 10-ft starute was used as wind sensor. The meteorological variable values were reported at irregular intervals and interpolated to 1-km heights by computer.

The region of interest was between 25 and 60 km. Results obtained for Kourou above 70 km are doubtful, since errors in temperature and winds at these levels are high. Harmonic analyses for temperature were not carried out for Natal, Fort Churchill, and Fort Sherman, since it was felt that due to much missing data the analyses would lack meaning. Also, since Wallops Island and Mar Chiquita had either too much data missing or data too irregularly spaced, no harmonic analyses were carried out for these stations. Harmonic analyses of winds (zonal and meridional components) were carried out for all remaining stations. Analyses of altitude distributions of meridional heat and zonal momentum transports were carried out for Natal, Kourou, Antigua, Ascension, Fort Sherman and Wallops Island. Also, mean variances of zonal and meridional winds in the vertical were calculated for these stations. These variances give an estimate of the intensity of turbulence.

Although such limited data do not allow for meaningful error analyses such as those described by Chapman and Lindzen (1970), the results do suggest some strong patterns. We hope that as more rocket data become available, statistically significant results will be obtained.

## INTERPOLATION AND HARMONIC ANALYSIS

As mentioned in the last section, since harmonic analysis requires equally spaced data, interpolation for missing data is necessary. Our analysis used 8 observations equally spaced at 3-hour intervals over a 24-hour period. The interpolation scheme chosen was the cubic spline. This method is described by Conte and deBoor (1965).

An interpolant which interpolates a function P and its first derivatives at the data points $t_i$ and $t_{i+1}$, t representing

time, may be given by

$$P(t) = \phi_1(G)P(t_i) + \phi_2(G)\Delta t_i P'(t_i) + \phi_3(G)P(t_{i+1}) +$$

$$\phi_4(G)\Delta t_i P'(t_{i+1}) \ ;$$

where:

$$G = \frac{t-t_i}{t_{i+1}-t_i}$$

$$\Delta t_i = t_{i+1} - t_i \ ;$$

$$\phi_1(G) = (G-1)^2(2G+1) \ ;$$

$$\phi_2(G) = (G-1)^2 G \ ;$$

$$\phi_3(G) = G^2(3-2G) \ ;$$

$$\phi_4(G) = G^2(G-1) \ .$$

In our case, i=1, 2,..., 7, 8. If we allow the first derivatives to be parameters and denote them by $S_i$ and $S_{i+1}$, we get for the interpolant

$$P(t) = \phi_1(G)P(t_i) + \phi_2(G)\Delta t_i S_i + \phi_3(G)P(t_{i+1}) +$$

$$\phi_4(G)\Delta t_i S_{i+1}.$$

Given a set of N data points, we impose a continuity in the second derivatives across the points $t_i$; and this gives a system of equations for the $S_i$. This system is obtained by differentiating the previous equation for interpolation over the time interval $[t_i, t_{i+1}]$ twice, and doing the same to the interpolant over $[t_{i-1}, t_i]$. The two equations are now evaluated at $t_i$ and are equated. The resulting equation is

$$\frac{S_{i-1}}{\Delta t_{i-1}} + 2S_i\left[\frac{1}{\Delta t_{i-1}} + \frac{1}{\Delta t_i}\right] + \frac{S_{i+1}}{\Delta t_i}$$

$$= \frac{1}{(\Delta t_i)^2}\left[-3P(t_i) + 3P(t_{i+1})\right] + \frac{1}{(\Delta t_{i-1})^2}\left[-3P(t_{i-1}) + 3P(t_i)\right]$$

This equation holds at interior points i=2,...,N-1. The P's are known function values. There are N-2 equations in N S's (unknowns). In our case, $\Delta t$=3 hours. Two more equations can be obtained by assuming $P''(T_1)=0$ and $P''(t_N)=0$. With these assumptions, we now have a tridiagonal system of N equations in the N unknowns, $S_1...,S_N$. The resulting system of equations can be readily solved by using the LU* method of matrix decomposition. Thus we obtain an interpolant which is continuous in second derivative across the interpolation points.

In our case the missing temperatures and winds were filled in by cubic spline interpolation, and the harmonic analysis was then applied after the trend in the data was removed. The trend removal was accomplished through use of a parabolic least-squares fit of the form.

$$P = a + bt + ct^2.$$

The procedure is described by Panofsky and Brier (1965).

The harmonic analysis used is that described by Panofsky and Brier (1965). Given N data points, a variate P may be described as the sum of its mean plus the sum of N/2 harmonics.

$$P = \overline{P} + \sum_{i=1}^{N/2}\left[A_i \sin\left(\frac{360^\circ}{F} i\, t\right) + B_i \cos\left(\frac{360^\circ}{F} i\, t\right)\right]$$

F represents the total period of the periodic function, which in our case is 24 hours, while N=8. The quantity i represents the number of the harmonic. For i+1 the period of the

*LU = lower and upper triangular decomposition

harmonic is 24 hours, while the semidiurnal and terdiurnal harmonics are represented by i=2 and i=3, respectively. The above harmonic coefficients are found by the following equations

$$A_i = \frac{2}{N} \sum_{j=1}^{N} \left[ P_j \sin\left(\frac{360^\circ}{F} i\, t\right) \right],$$

$$B_i = \frac{2}{N} \sum_{j=1}^{N} \left[ P_j \cos\left(\frac{360^\circ}{F} i\, t\right) \right],$$

where i=1,...,N/2-1. The A for the last harmonic (N/2) is zero, while the B for this harmonic is as above but divided by 2.

The A's and B's are combined to give the amplitude $C_i$, where

$$C_i = \sqrt{A_i^2 + B_i^2},$$

since

$$C_i \cos\left[\frac{360^\circ i}{F} (t - t_i)\right] = A_i \sin\left(\frac{360^\circ}{F} i\, t\right) + B_i \cos\left(\frac{360^\circ}{F} i\, t\right).$$

The phase angle or hour of maximum, $t_i$, of the harmonic can be uniquely determined by the relationships

$$t_i = \frac{F}{360^\circ i} \sin^{-1}(A_i/C_i)$$

and

$$t_i = \frac{F}{360^\circ i} \tan^{-1}(A_i/B_i).$$

The first three harmonics for temperature, meridional wind and zonal wind oscillations were calculated for the selected stations at 1-km intervals. The range of altitudes,

for which amplitudes and phase angles were calculated, varies from station to station due to data irregularities; however, the typical range was 25 to 60 km.

The question arose as to what effect the cubic spline interpolation had on the harmonic coefficients and phase angles. Data from Kourou, French Guiana helped answer this question. Since a complete set of data was available at Kourou for temperature and zonal and meridional winds, it was a simple matter to see how removing a set of data and replacing it with interpolated data would affect the outcome of the harmonic analysis. As often was the case, two consecutive temperature soundings were missing, while in all cases, only 1 interpolation at each altitude was necessary for zonal and meridional winds. Various time intervals were removed and filled in with interpolated data. Figure 1 shows amplitudes for the diurnal oscillations of temperature along with those of zonal and meridional winds for the complete set of data at Kourou. The dashed curves represent amplitudes for the interpolated sets. Two consecutive soundings were replaced by interpolation for the temperature oscillation, while only one set was replaced for the wind oscillations. The results for zonal and meridional wind diurnal oscillations obtained from the set with the interpolated sounding as opposed to results from the complete set show little difference. Results for the interpolated set show amplitudes which are slightly larger than those obtained for the complete set. For the diurnal temperature oscillation, the difference in the analyses for the two sets of data is greater due to the fact that 2 consecutive soundings were replaced; however, the shapes of altitude distributions of amplitude are approximately the same except in the 40 to 50 km region where the difference is large. Similar results were obtained for phases.

Thus it is seen that replacement of one sounding by cubic spline interpolation does not drastically affect the harmonic analysis. Similar results were obtained for the semidiurnal and terdiurnal components. With regards to temperature

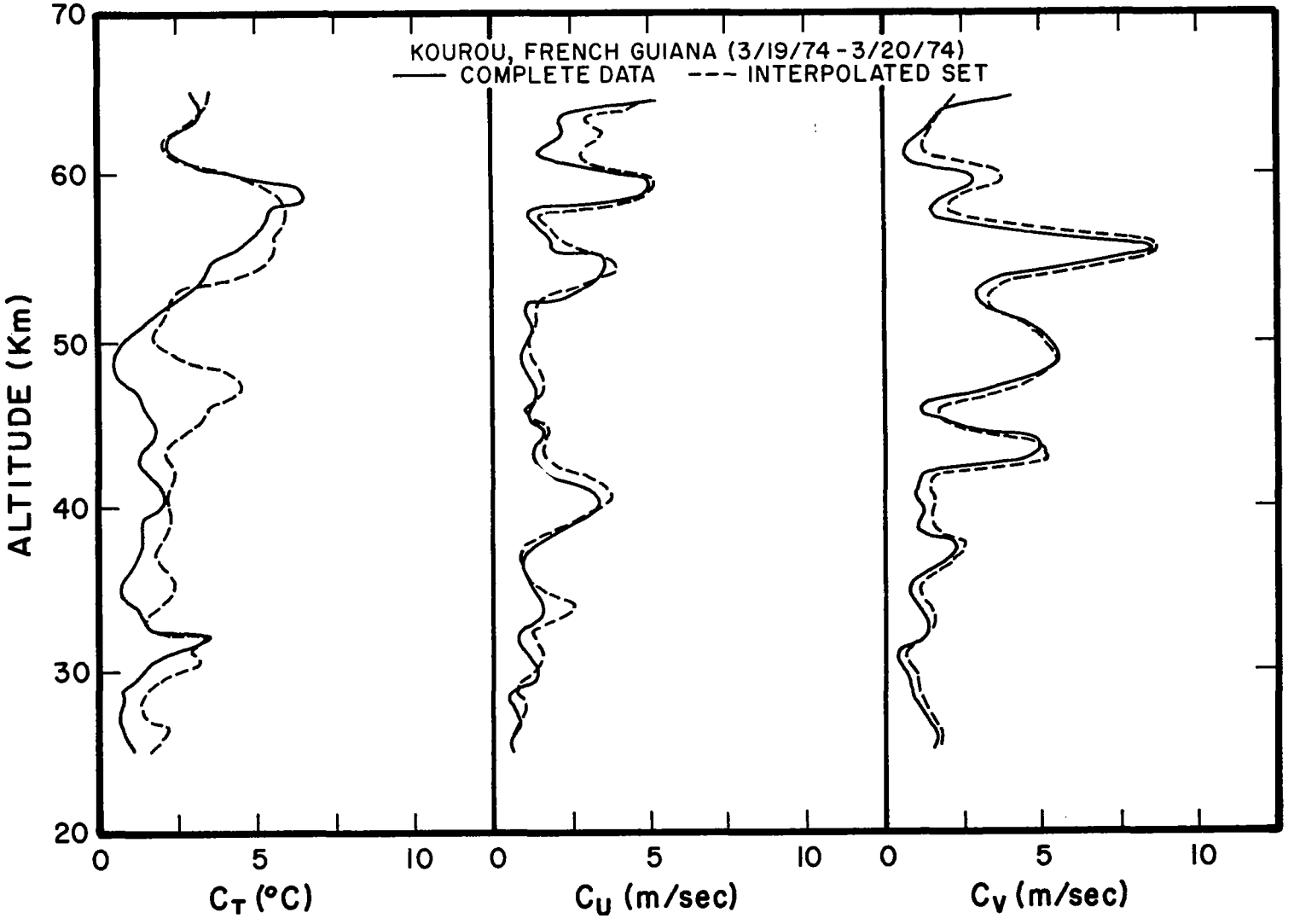


Fig. 1. Comparison between solar diurnal amplitudes for temperature and zonal and meridional wind oscillations obtained from a complete set of diurnal data, and the amplitudes obtained from the same data but with certain portions of data replaced with interpolated (cubic spline) data.

oscillation, the results which follow are rough estimates.

## WIND STRUCTURE IN THE STRATOSPHERE AND MESOSPHERE ON 19-20 MARCH 1974

Figure 2 shows mean profiles at Kourou on 19-20 March 1974 for temperature, and zonal and meridional winds. The mean position of the stratopause occurs around 42 km, reaching a maximum temperature of $0^{o}C$ at this altitude. The region of the thermal decline into the mesosphere begins around 52 km. The zonal wind reaches a maximum at Kourou of around 45 m/s at about 68 km. This feature is quite interesting, since in routine soundings taken in early March and February 1974 at Kourou, winds in the upper mesosphere are substantially lower. Large mesospheric wind fluctuations have been known for some time, and their cause has never been fully explained. One possible cause is the interaction of vertically propagating waves with critical levels as outlined by Booker and Bretherton (1967).

Figures 3 and 4 show respectively the latitudinal cross sections for zonal and meridional winds. The data of 19-20 March 1974 was used for these graphs. These figures are courtesy of NASA (Wallops Island). A persistent core of easterly winds around 50 km over $9^{o}N$ is seen. This appears prominent in Figure 3. In the northern mid-latitude stratosphere, winds are strongly westerly, while the tropical stratosphere shows predominantly easterly winds. Both northern mid-latitude and tropical mesospheric regions show regions of strong westerly winds with a maximum of 65 m/s over the equator at 65 km. In the southern hemispheric stratosphere, winds tend to be easterly to $40^{o}S$.

In Figure 4 we see the meridional winds tending to be very weak in the northern and southern hemisphere stratospheric regions; however, in the northern hemisphere mesosphere, meridional winds are essentially northerly, and in the southern hemisphere mesosphere these winds are southerly. In the

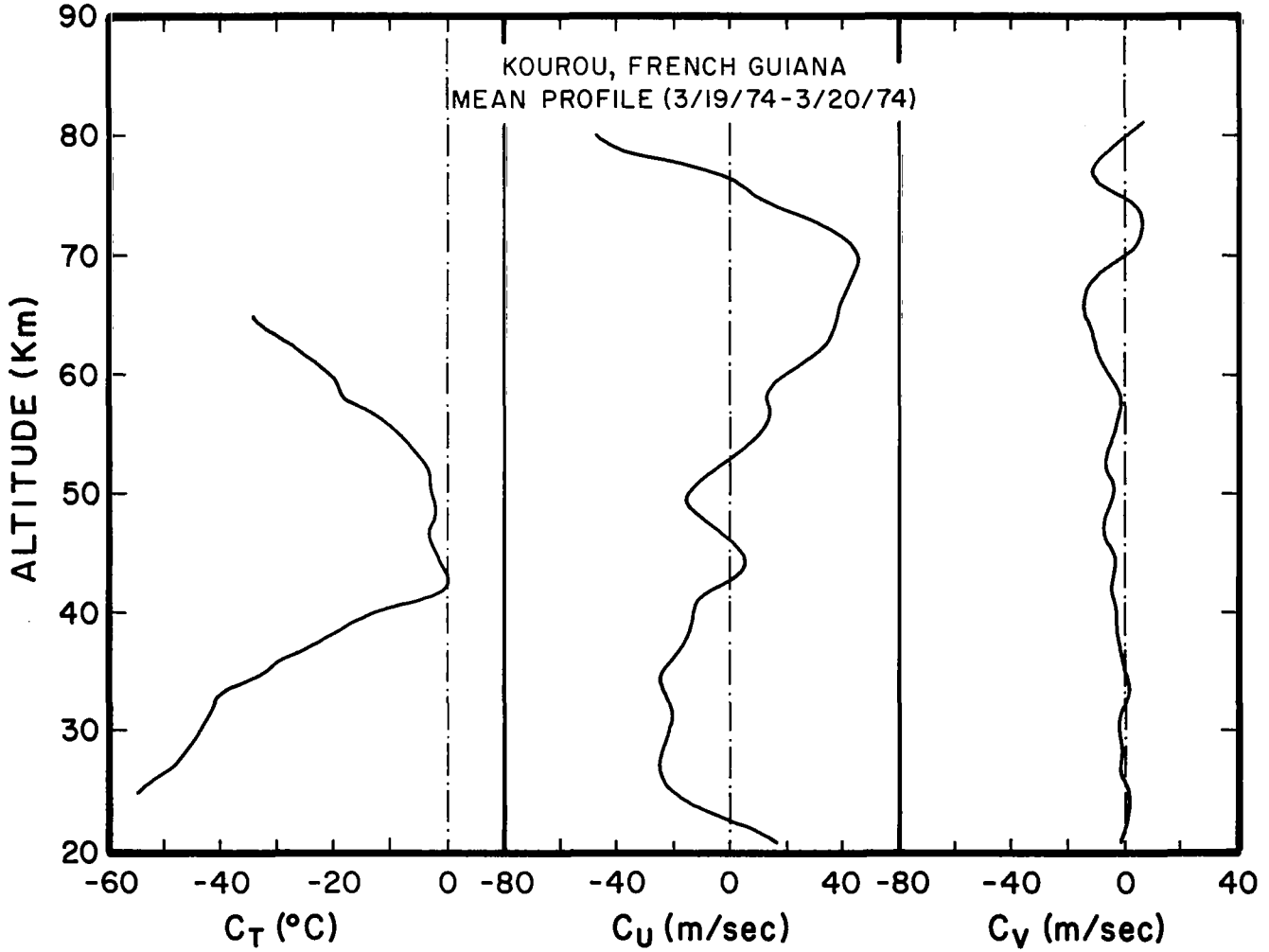


Fig. 2. Mean profiles of temperature and zonal and meridional winds at Kourou.

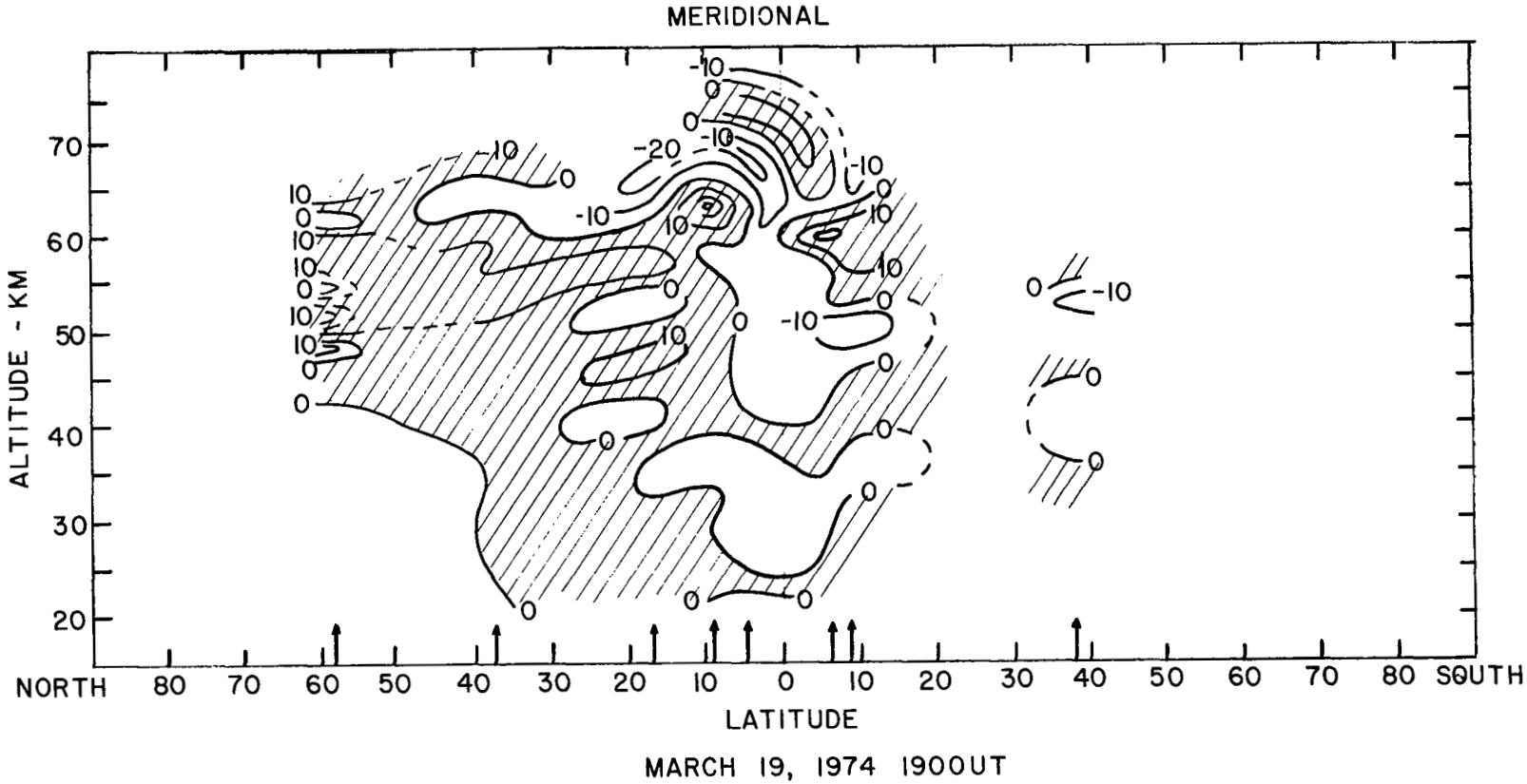


Fig. 3. Latitude cross section of zonal winds with altitude. Courtesy NASA (Wallops Island).

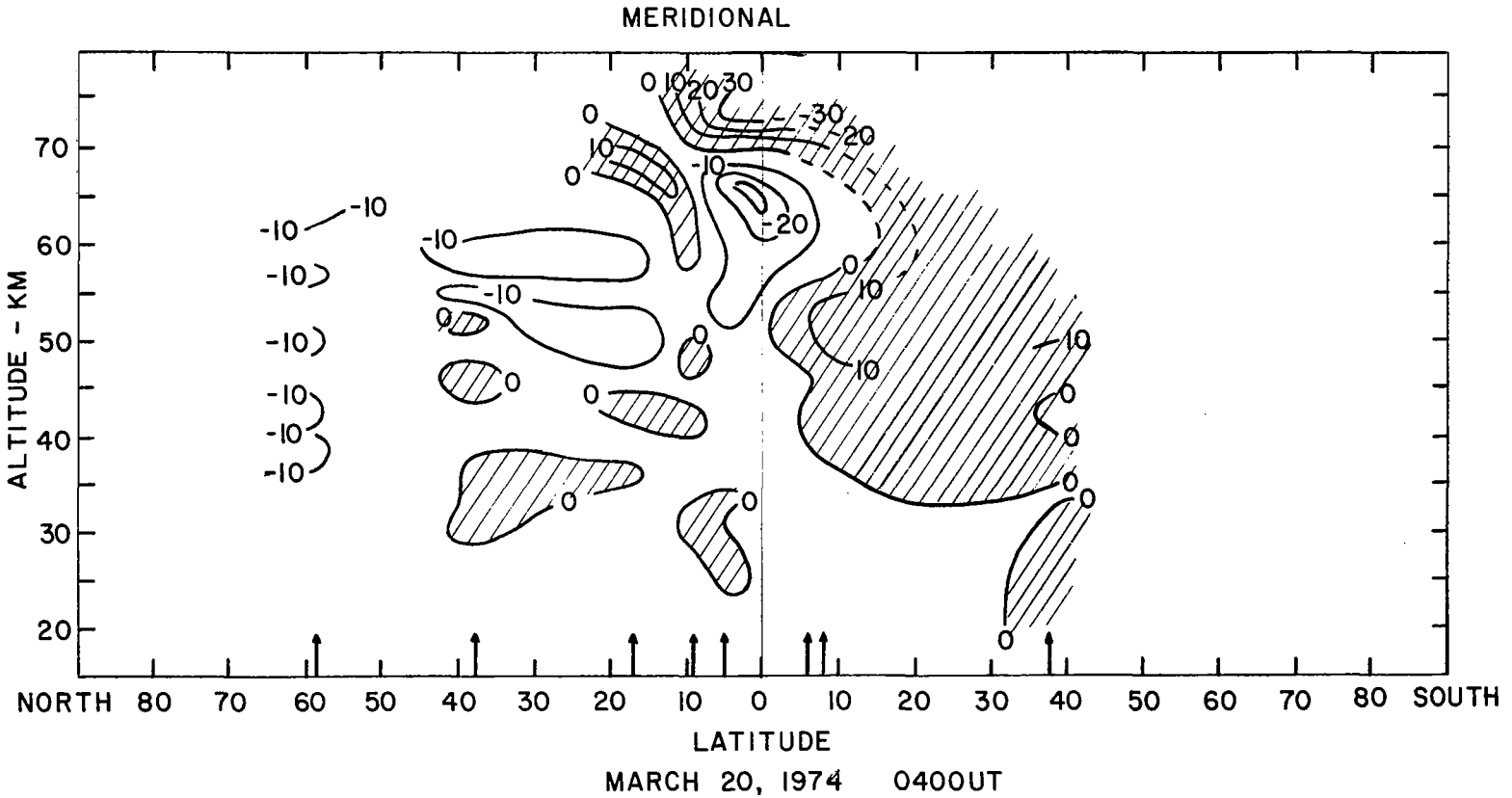


Fig. 4. Latitude cross section of meridional winds with altitude. Courtesy NASA (Wallops Island).

upper mesosphere over the equator the meridional winds increase substantially, being northerly between 55 and 67 km at 10 to 20 m/s, and southerly above 67 km increasing in magnitude to 30 m/s at 70 km.

Figure 5 shows a time cross section of meridional winds for Kourou during the period 19-20 March 1974. From this cross section, the oscillatory nature of the meridional wind is clearly seen, the amplitude of oscillation increasing with height rapidly above 50 km.

## TURBULENT TRANSPORT OF HEAT AND ZONAL MOMENTUM

Figures 6, 7 and 8 show altitude distributions of variance of temperature (T), and zonal (U) and meridional (V) winds for six stations. As might be expected, the variances in general increase with height; hence, turbulent energy per unit mass is increasing with height. There is relatively less increase at Antigua and Fort Sherman. All stations show an initial maximum of variance for temperature and winds in the vicinity of ozone layer (40-45km) maximum heating. The coupling between ozone layer heating and the dynamics seems obvious.

Figures 9, 10 and 11 show altitude distributions of turbulent meridional transport of heat and zonal momentum. There is a general increase with height of the meridional heat and zonal momentum transports. Wallops Island has the largest values of $\overline{T'V'}$ and $\overline{U'V'}$. For Wallops, $\overline{T'V'}$ is positive between 43 and 60 km. This indicates a northward heat transport. More graphs such as these using longer records are needed in order to establish heat and momentum transport characteristics of the tropical and mid-latitude stratospheric and mesospheric regions.

Tables 1 and 6 show the mean variances of zonal and meridional wind in the vertical for six stations. This method was used by Kao and Sands (1966) to examine the intensity of

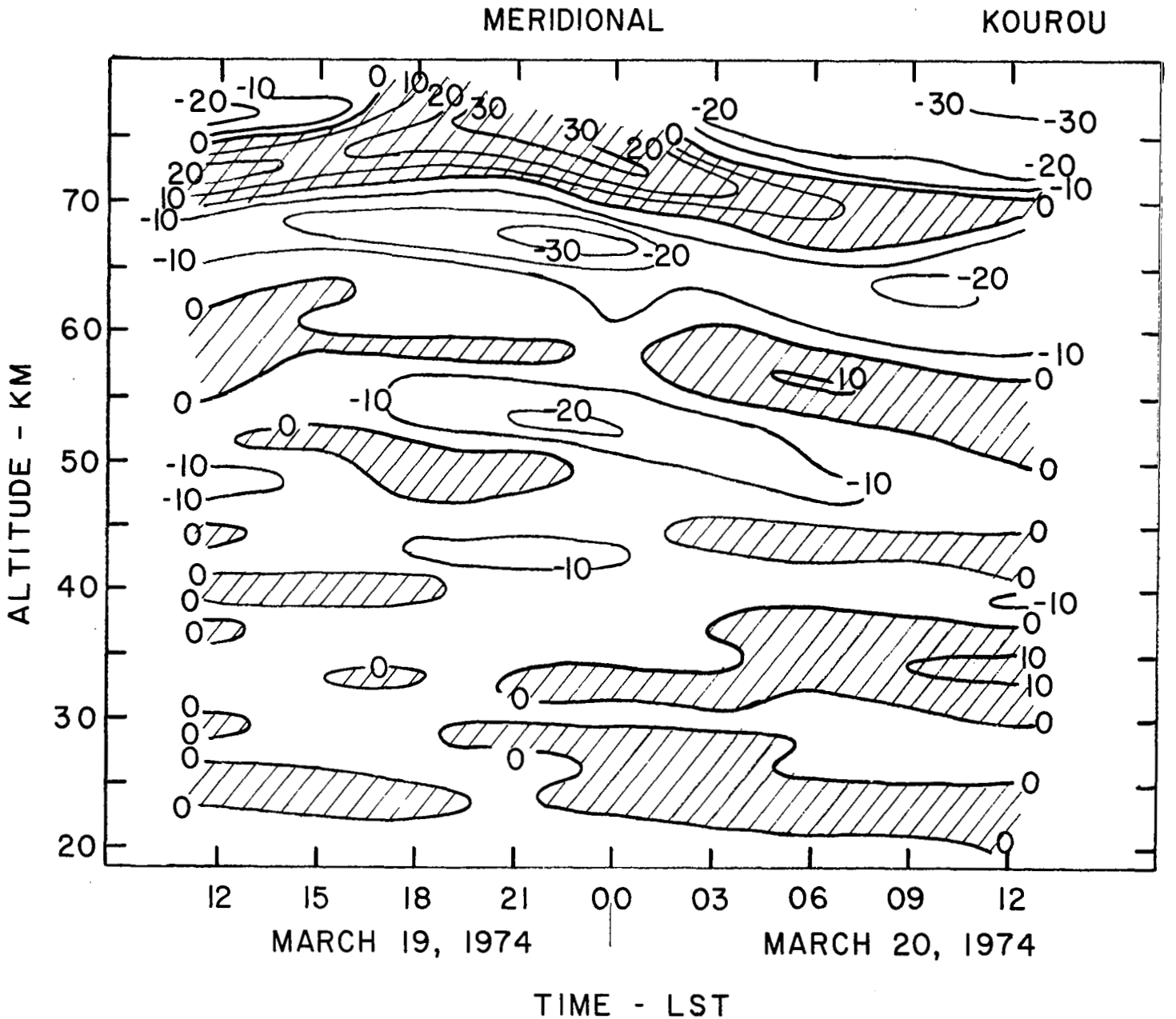


Fig. 5. Time cross section of winds with altitude over Kourou, French Guiana. Courtesy NASA (Wallops Island).

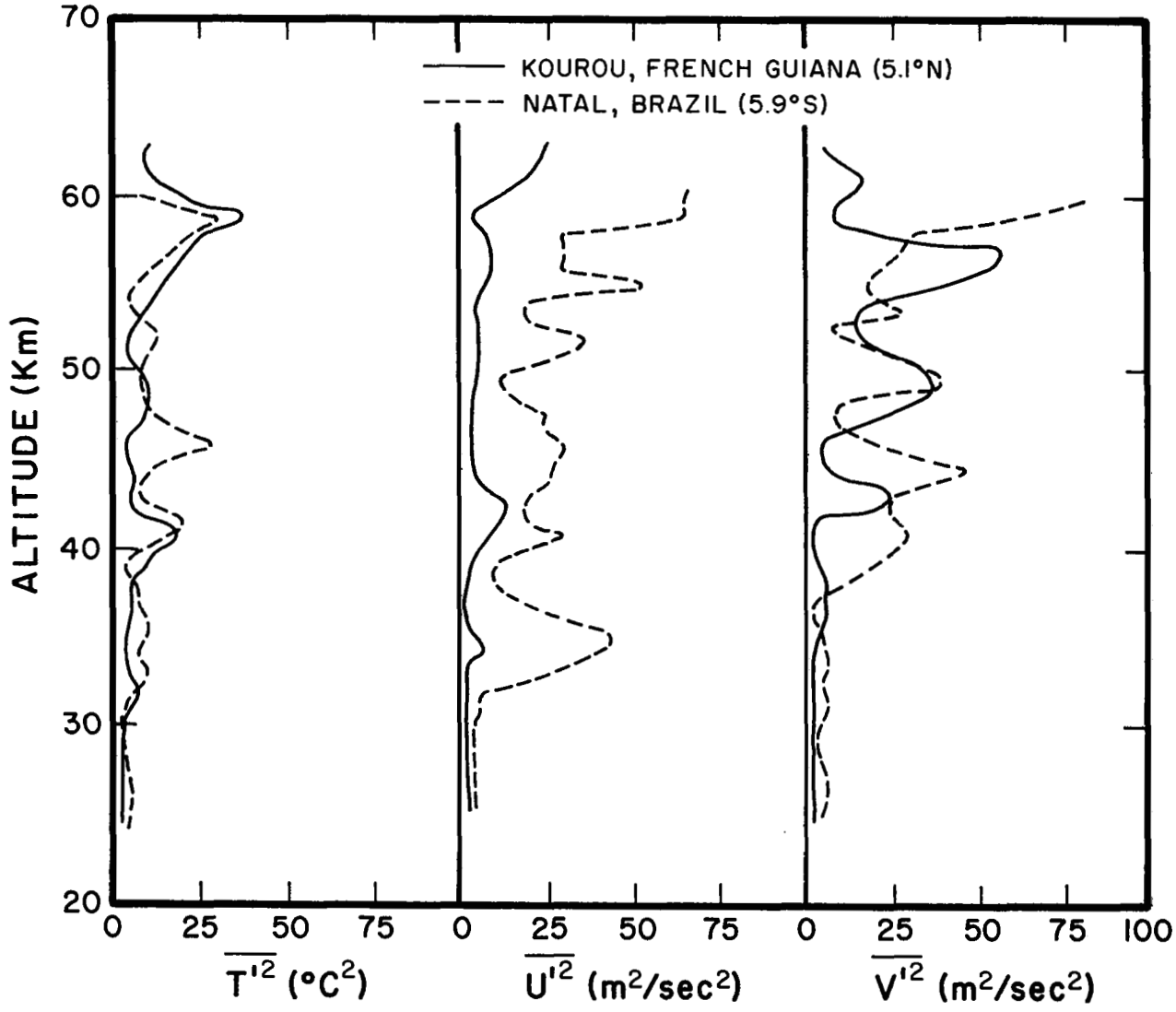


Fig. 6. Altitude distribution of variances of temperature, zonal wind and meridional wind for 19-20 March 1974.

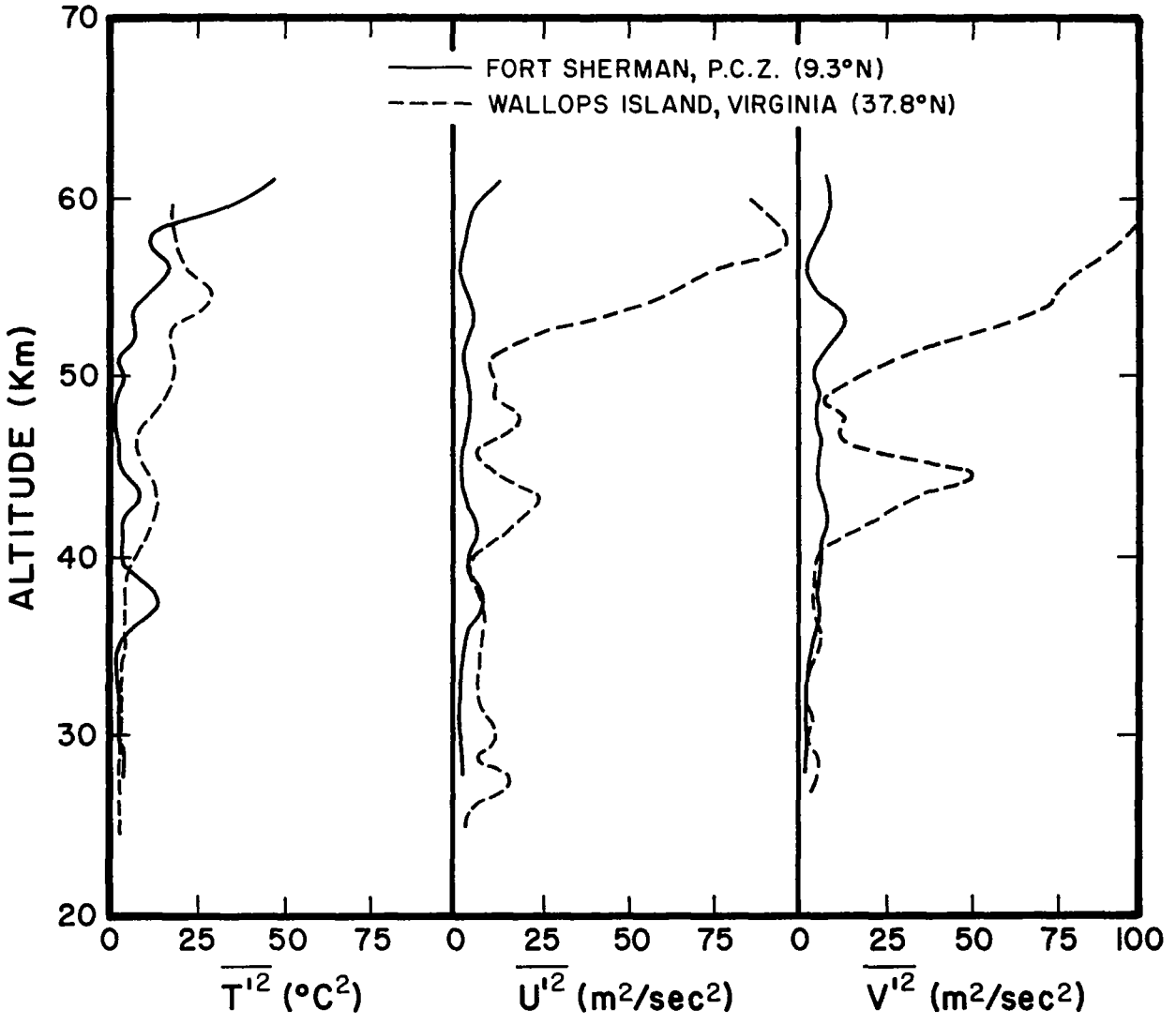


Fig. 7. Altitude distributions of variances of temperature, zonal wind and meridional wind for 19-20 March 1974.

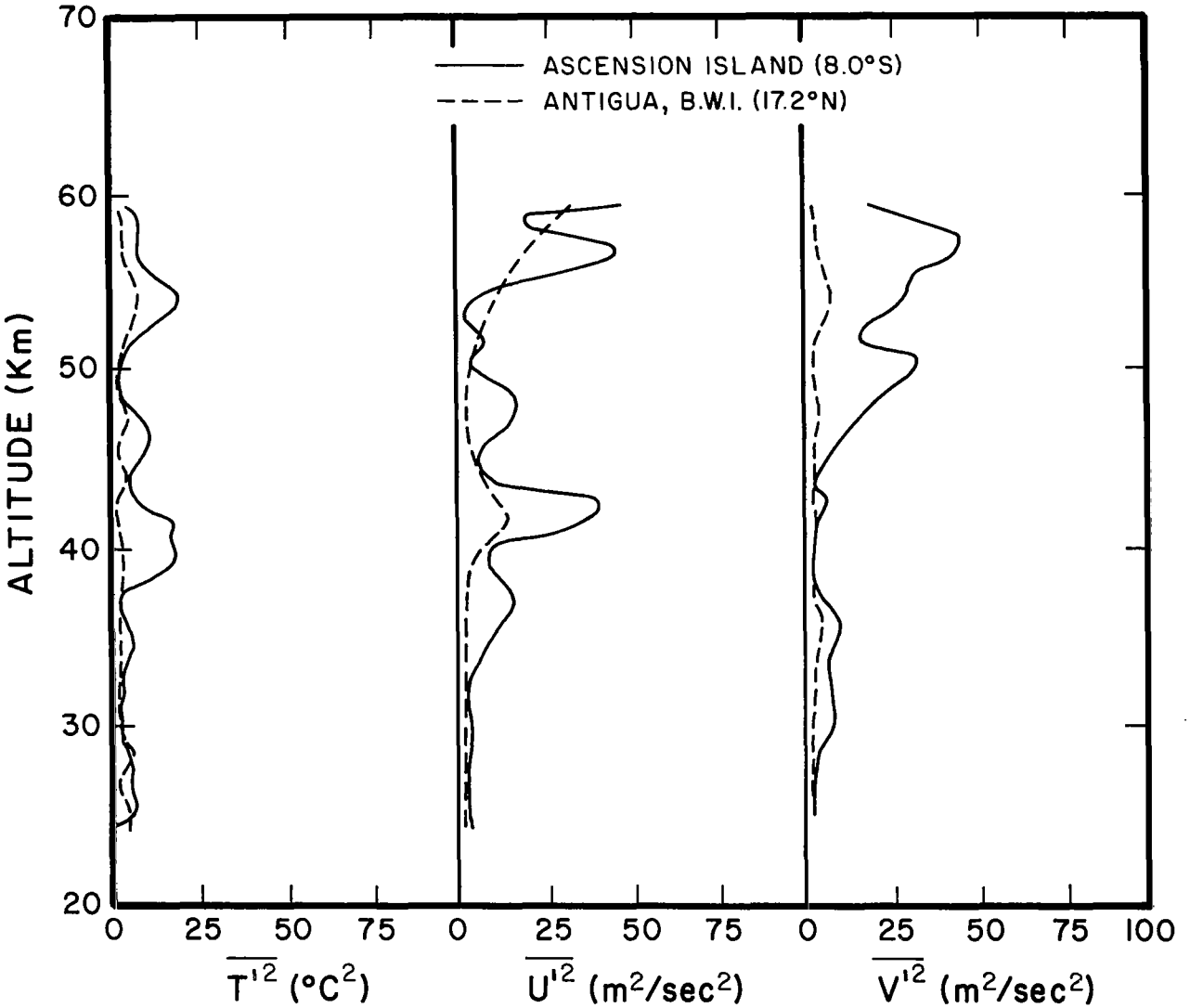


Fig. 8. Altitude distributions of variances of temperature, zonal wind and meridional wind for 19-20 March 1974.

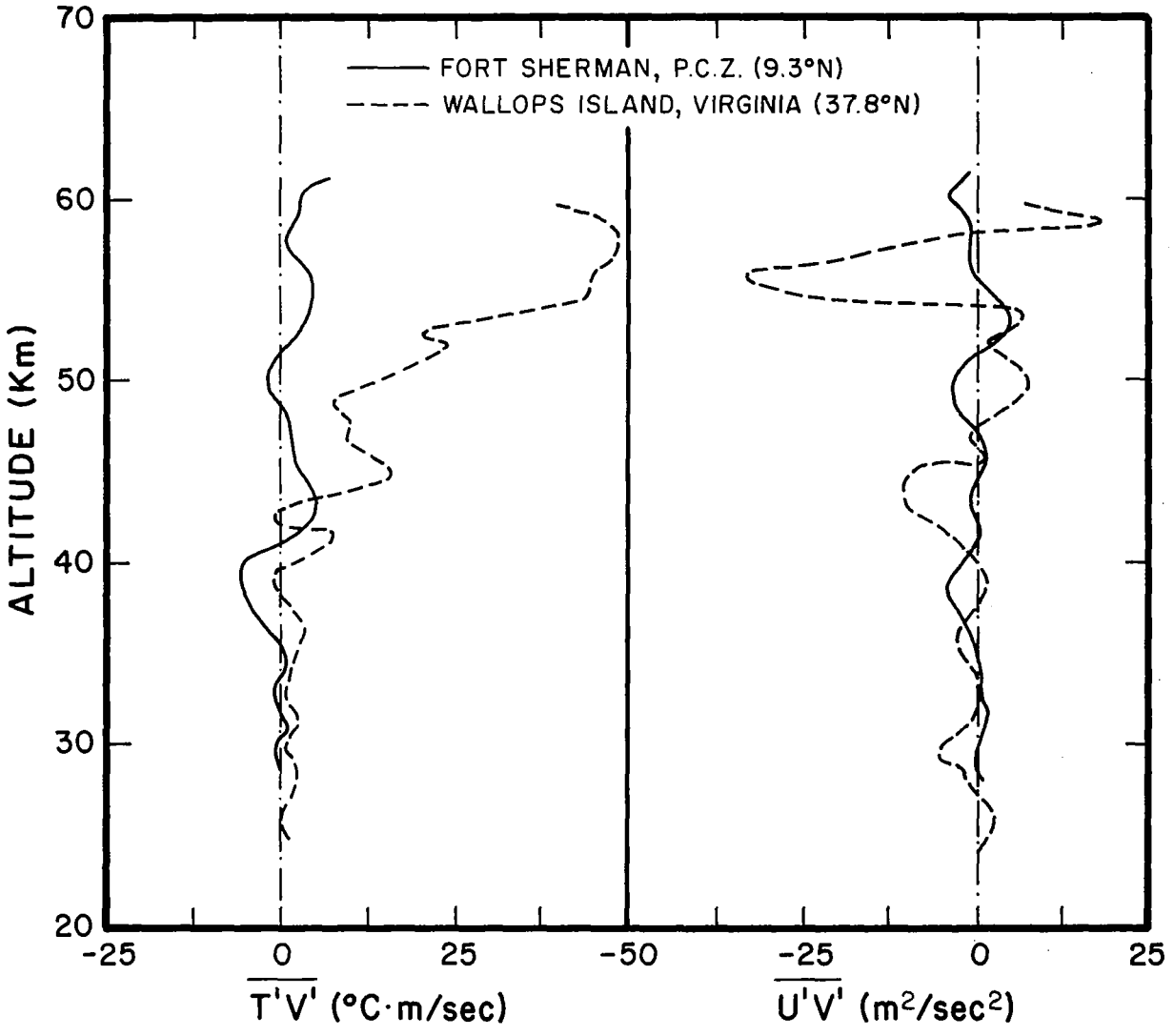


Fig. 9. Altitude distributions of meridional heat transport and meridional transport of zonal momentum for 19-20 March 1974.

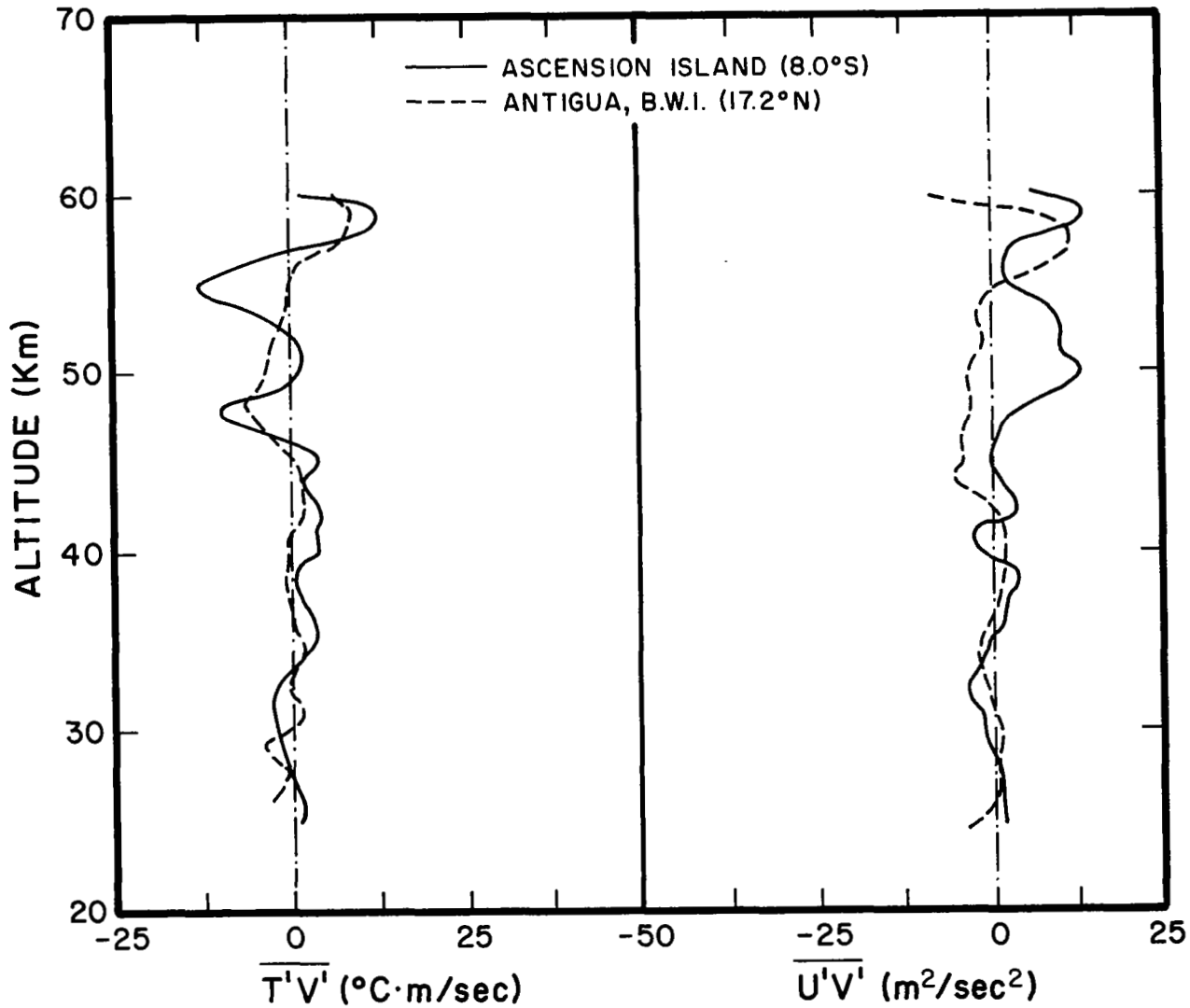


Fig. 10. Altitude distributions of meridional heat transport and meridional transport of zonal momentum for 19-20 March 1974.

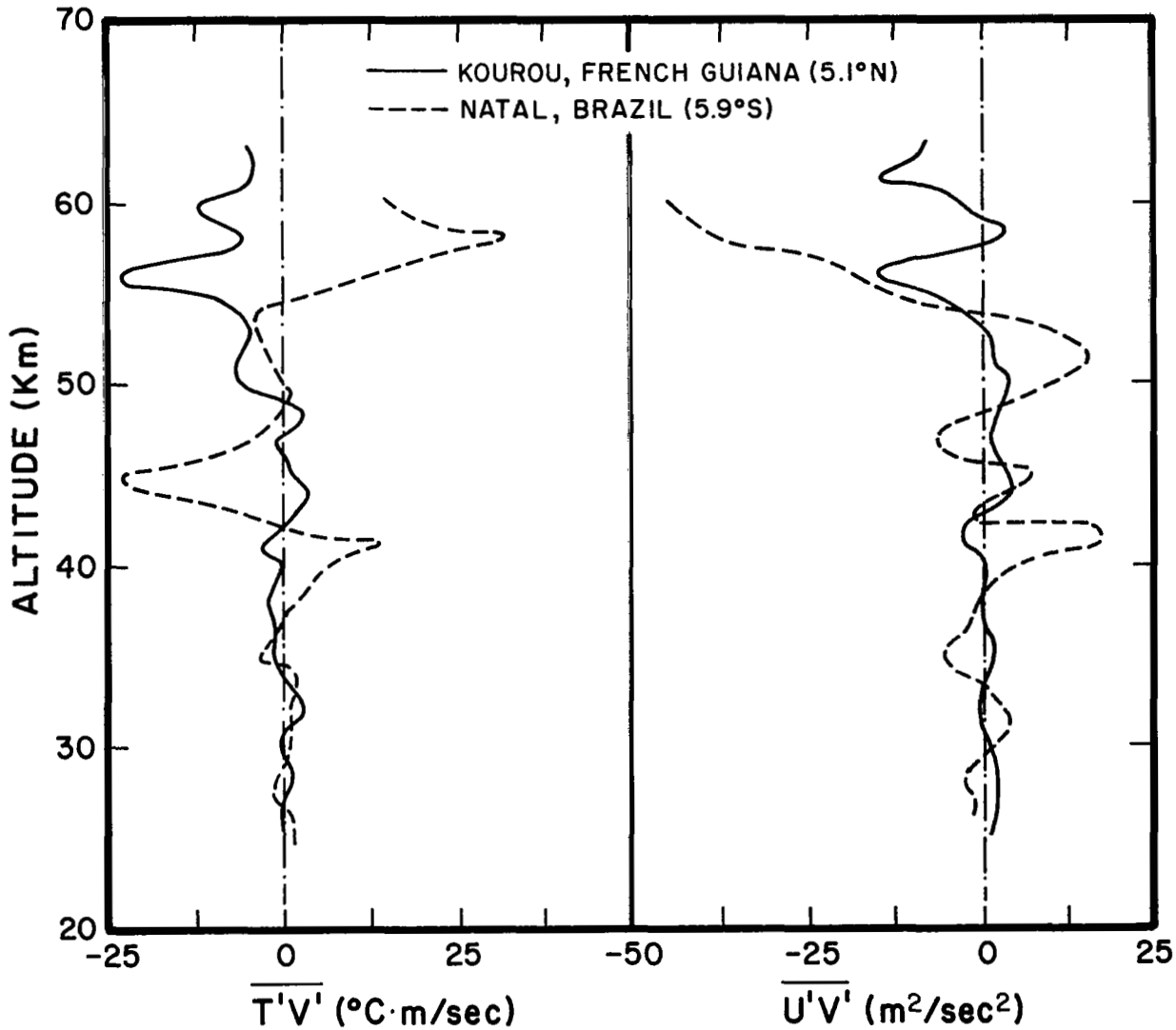


Fig. 11. Altitude distributions of meridional heat transport and meridional transport of zonal mementum for 19-20 March 1974.

turbulence. The zonal component of turbulent energy is exceeded by the meridional component at Wallops, Kourou, Antigua and Fort Sherman. In all cases, total turbulent energy varies greatly throughout the day. It is interesting to note that even though $\bar{V}$ was small in most cases at most heights, V itself was not of negligible magnitude at all times. Thus, large variations in the meridional wind component are noted, and as seen from the variances of V in the vertical, turbulent energy due to the meridional component is quite significant.

Using 30 and 15 hours as the averaged integral time scale for the zonal and meridional component of the turbulent motion in the upper atmosphere respectively, the zonal and meridional components of the eddy diffusivity at Kourou and Wallops Island are estimated to be

| | $K_{xx}(m^2sec^{-1})$ | $K_{yy}(m^2sec^{-1})$ |
|---|---|---|
| Kourou | $4 \times 10^6$ | $3 \times 10^6$ |
| Wallops Island | $3 \times 10^6$ | $1.6 \times 10^6$ |

which indicates that the horizontal eddy diffusivity in the equatorial upper stratosphere is almost twice that in the mid-latitude upper stratosphere, which is quite significant. Because of the sparse rocket data, the above values of $K_{xx}$ and $K_{yy}$ can only be considered as a rough estimation of the order of magnitude of the horizontal eddy diffusivity. To determine the exact value of the diffusivity, a large number of wind measurements will be needed.

## RESULTS OF HARMONIC ANALYSIS

Tidal theory is examined in detail by Chapman and Lindzen (1970). The theory involves 4 basic limitations:

1) Tides are assumed linear perturbations of basic state.

2) Horizontal variations in the mean basic temperature and pressure along with mean motions are ignored.

3) All dissipative mechanisms are ignored.

4) Topography ignored. The earth is assumed spherical,

| Date | Time | $[V'^2]$ ($m^2sec^{-2}$) | $[U'^2]$ ($m^2sec^{-2}$) |
|---|---|---|---|
| 3/19/74 | 1605Z | 49.78 | 42.99 |
| 3/19/74 | 1954Z | 49.37 | 10.63 |
| 3/19/74 | 2200Z | 28.09 | 27.52 |
| 3/20/74 | 0047Z | 25.48 | 41.20 |
| 3/20/74 | 0108Z | 29.99 | 43.57 |
| 3/20/74 | 0453Z | 46.78 | 12.62 |
| 3/20/74 | 0706Z | 25.39 | 17.37 |
| 3/20/74 | 1000Z | 22.19 | 31.95 |
| 3/20/74 | 1040Z | 26.67 | 19.12 |
| 3/20/74 | 1240Z | 53.77 | 43.06 |
| 3/20/74 | 1639Z | 37.49 | 17.59 |

$([V'^2]) = 35.90$ $([U'^2]) = 27.96$

( ) : Time Average

[ ] : Average over Height

V : Meridional Wind

U : Zonal Wind

TABLE 1. Mean square zonal and meridional components of the turbulent velocity at Wallops Island, Virginia

| Date | Time | $[V'^2]$ $(m^2sec^{-2})$ | $[U'^2]$ $(m^2sec^{-2})$ |
|---|---|---|---|
| 3/19/74 | 1500Z | 8.29 | 4.86 |
| 3/19/74 | 1800Z | 9.74 | 3.88 |
| 3/19/74 | 2100Z | 12.21 | 21.41 |
| 3/20/74 | 0000Z | 23.43 | 6.01 |
| 3/20/74 | 0300Z | 15.85 | 11.18 |
| 3/20/74 | 0600Z | 23.78 | 14.30 |
| 3/20/74 | 0900Z | 28.09 | 11.00 |
| 3/20/74 | 1200Z | 8.85 | 6.25 |
| 3/20/74 | 1500Z | 18.13 | 5.19 |

$(\overline{[V'^2]}) = 16.49$ $\quad$ $(\overline{[U'^2]}) = 9.34$

( ) : Time Average

[ ] : Average over Altitude

V : Meridional Wind

U : Zonal Wind

TABLE 2. Mean square zonal and meridional components of the turbulent velocity at Kourou, French Guiana

| Date | Time | $[V'^2]$ $(m^2sec^{-2})$ | $[U'^2]$ $(m^2sec^{-2})$ |
|---|---|---|---|
| 3/19/74 | 1600Z | 19.89 | 10.86 |
| 3/19/74 | 1900Z | 25.22 | 11.62 |
| 3/19/74 | 2200Z | 20.78 | 13.82 |
| 3/20/74 | 0100Z | 15.33 | 17.76 |
| 3/20/74 | 0400Z | 12.52 | 19.90 |
| 3/20/74 | 0700Z | 15.57 | 30.11 |
| 3/20/74 | 1000Z | 12.83 | 21.88 |
| 3/20/74 | 1303Z | 8.81 | 5.56 |
| 3/20/74 | 1600Z | 5.85 | 10.15 |

$(\overline{[V'^2]}) = 15.20$ $\quad$ $(\overline{[U'^2]}) = 15.74$

( ) : Time Average

[ ] : Average over Altitude

V : Meridional Wind

U : Zonal Wind

TABLE 3. Mean square zonal and meridional components of the turbulent velocity at Ascension Island

| Date | Time | $[V'^2]$ $(m^2sec^{-2})$ | $[U'^2]$ $(m^2sec^{-2})$ |
|---|---|---|---|
| 3/19/74 | 1501Z | 10.60 | 9.47 |
| 3/19/74 | 1820Z | 19.42 | 5.93 |
| 3/19/74 | 2100Z | 16.32 | 16.14 |
| 3/20/74 | 0000Z | 16.23 | 3.37 |
| 3/20/74 | 0300Z | 14.70 | 11.17 |
| 3/20/74 | 0600Z | 13.59 | 9.49 |
| 3/20/74 | 0900Z | 23.95 | 6.79 |
| 3/20/74 | 1200Z | 5.83 | 3.37 |
| 3/20/74 | 1500Z | 10.94 | 3.91 |

$([V'^2])$ = 14.62 $([U'^2])$ = 7.74

( ) : Time Average

[ ] : Average over Altitude

V : Meridional Wind

U : Zonal Wind

TABLE 4. Mean square zonal and meridional components of the turbulent velocity at Antigua, British West Indies

| Date | Time | $[V'^2]$ $(m^2sec^{-2})$ | $[U'^2]$ $(m^2sec^{-2})$ |
|---|---|---|---|
| 3/19/74 | 1600Z | 1.68 | 2.15 |
| 3/19/74 | 1900Z | 2.29 | 3.38 |
| 3/19/74 | 2200Z | 6.43 | 3.53 |
| 3/20/74 | 0100Z | 2.69 | 2.61 |
| 3/20/74 | 0400Z | 5.14 | 5.31 |
| 3/20/74 | 0700Z | 8.86 | 3.43 |
| 3/20/74 | 1015Z | 9.48 | 4.62 |
| 3/20/74 | 1315Z | 3.69 | 2.08 |

$([V'^2]) = 5.04$ $([U'^2]) = 3.39$

( ) : Time Average

[ ] : Average over Altitude

V : Meridional Wind

U : Zonal Wind

TABLE 5. Mean square zonal and meridional components of the turbulent velocity at Fort Sherman, Panama Canal Zone

| Date | Time | $[V'^2]$ $(m^2sec^{-2})$ | $[U'^2]$ $(m^2sec^{-2})$ |
|---|---|---|---|
| 3/19/74 | 1600Z | 24.66 | 31.51 |
| 3/19/74 | 1900Z | 45.86 | 37.34 |
| 3/20/74 | 0100Z | 27.02 | 34.53 |
| 3/20/74 | 0748Z | 18.23 | 27.98 |
| 3/20/74 | 1000Z | 9.78 | 22.17 |
| 3/20/74 | 1321Z | 16.13 | 20.61 |
| 3/20/74 | 1600Z | 6.47 | 50.59 |

$([V'^2])$ = 21.16 $([U'^2])$ = 32.10

( ) : Time Average

V : Meridional Wind

U : Zonal Wind

TABLE 6. Mean square zonal and meridional components of the turbulent velocity at Natal, Brazil

and longitudinal variations of absorbing gases are neglected. From the linearized governing equations LaPlace's tidal equation and a vertical structure equation are obtained. These are solved subject to the proper thermotidal forcing. The main thermal excitation source for solar tides appears to be due to insolation absorption by ozone and water vapor. In general, gravitational excitation is much weaker than thermal excitation. Lindzen and Hong (1974) have updated the general theory through the inclusion of mean winds and horizontal temperature gradients with Rayleigh friction.

The linearized governing equations for tidal perturbations are:

$$\frac{\partial u}{\partial t} - 2\omega v \cos\theta = -\frac{1}{a}\frac{\partial}{\partial \theta}\left(\frac{\delta P}{\rho_o}\right),$$

$$\frac{\partial v}{\partial t} + 2\omega u \cos = -\frac{1}{a \sin\theta}\frac{\partial}{\partial \phi}\left(\frac{\delta P}{\rho_o}\right),$$

$$\frac{\partial \delta P}{\partial z} = -g\delta\rho ,$$

$$\frac{\partial \delta\rho}{\partial t} + w\frac{d\rho_o}{dz} = -\rho_o \vec{\nabla}\cdot\vec{\nabla} ,$$

$$C_v\left(\frac{\partial \delta T}{\partial t} + w\frac{dT_o}{dz}\right) = -gH\vec{\nabla}\cdot\vec{\nabla} + J,$$

$$\frac{\delta P}{P_o} = \frac{\delta T}{T_o} + \frac{\delta\rho}{\rho_o} .$$

In the above equations, the symbols are:

- $\theta$ co-latitude
- $\phi$ longitude
- z altitude
- a radius of the earth

$\omega$ earth's angular velocity

$u$ velocity in the $\theta$ direction

$v$ velocity in the $\phi$ direction

$w$ vertical velocity

$\delta T$ temperature perturbation

$\delta \rho$ density perturbation

$\delta P$ pressure perturbation

$J$ thermotidal heating per unit mass per unit time

$T_o$ basic temperature field

$\rho_o$ basic density field

$P_o$ basic pressure field

$H$ $RT_o/g$

$R$ gas constant

$C_v$ heat capacity at constant volume

Equations (1) and (2) involve the northerly and westerly momentum respectively. Equation (3) is the hydrostatic equation. Equation (4) is the continuity equation. Equation (5) is the thermodynamic energy equation, and Equation (6) is the perfect gas law.

A vertical distribution of $T_o(z)$ is assumed, with density and pressure related to temperature through the following equations:

$$P_o = P_o(0) \exp\left[-\int_o^z \frac{dz}{H}\right],$$

$$\rho_o = P_o/(gH).$$

Solutions are sought of the form

$$f(\theta, z(e^{i(\sigma t+s\phi)},$$

where $\sigma = 2n\pi(1 \text{ solar day})^{-1}$, $n=1,2,\ldots$ . $s$ is the zonal wave number $0, \pm 1, \pm 2, \ldots$ .

The above governing equations are now reduced to a single equation in the variable

$$Y = - \frac{1}{\gamma \sqrt{P_o P_o(0)}} \frac{DP}{Dt} .$$

$$\gamma = C_p / C_v$$

The vertical coordinate is replaced by

$$x = \int_o^z \frac{dz}{H} .$$

The single equation in y is separable in terms of its x and $\theta$ dependence, and we assume

$$Y = \sum_n Y_n(x) \Theta_n(\theta) .$$

After substitution for y we obtain LaPlace's tidal equation

$$F[\Theta_n] = - \frac{4a^2\omega^2}{g h_n} \Theta_n ,$$

where F is a differential operator. $h_n$ is known as the equivalent depth. $\Theta_n$ is to be bounded at the poles, and hence LaPlace's tidal equation is an eigenfunction-eigenvalue problem where the set of functions $\Theta_n$ are the eigenfunctions (Hough functions) with the set of $h_n$ the eigenvalues. The set $\{\Theta_n\}$ is orthogonal.

After expanding $J(x,\theta)$ in the form

$$J = \sum_n J_n(x) \Theta_n(\theta)$$

an equation for the vertical structure is obtained and is given by

$$\frac{d^2Y_n}{dx^2} + \frac{1}{h_n}\left(\kappa H + \frac{dH}{dx}\right) - \frac{1}{4}\ Y_n = \frac{\kappa J_n}{\gamma g h_n} e^{-x/2} ,$$

where $\kappa=(\gamma-1)/\gamma$. The above differential equation is a boundary value problem involving two boundary conditions at z=0 and $z\to\infty$. At z=0 it is assumed that w=0. It is usually assumed that $y_n$ remains bounded as $x\to\infty$.

The above treatment is taken from Lindzen (1970). Chapman and Lindzen (1970) describe detailed solutions to the tidal equation and vertical structure equation. Once these solutions are obtained, zonal and meridional wind components and temperatures may be obtained.

Figures 12 to 20 show the results of harmonic analysis for the stations previously mentioned. The diurnal and semidiurnal components are shown in Figures 12 to 17. In these figures, the subscript T stands for temperature, U for zonal wind and V for meridional wind.

As can be seen in Figures 12 to 17, the semidiurnal wind oscillations are mostly of equal magnitude and often exceed the diurnal oscillations. Reed (1967) found that in the region between 30 and 60 km the diurnal oscillation appears to be the main contributor to the meridional wind oscillation. In this study, however, the semidiurnal component of the zonal and meridional wind is as important as the diurnal oscillation and often exceeds it. At all stations both the diurnal and semidiurnal oscillations increase with altitude, starting in general at 1.5 to 2.5 m/s at 25 km reaching values of 5-8 m/s at 60 km. Fort Churchill and Fort Sherman appear to be exceptions. For Fort Churchill (57.1°N) the semidiurnal oscillation for both zonal and meridional winds reaches 15 m/s at 60 km. At Fort Sherman (9.3°N) the amplitudes of both diurnal and semidiurnal wind oscillations are much lower, being only about 1 m/s and 2 m/s for the diurnal

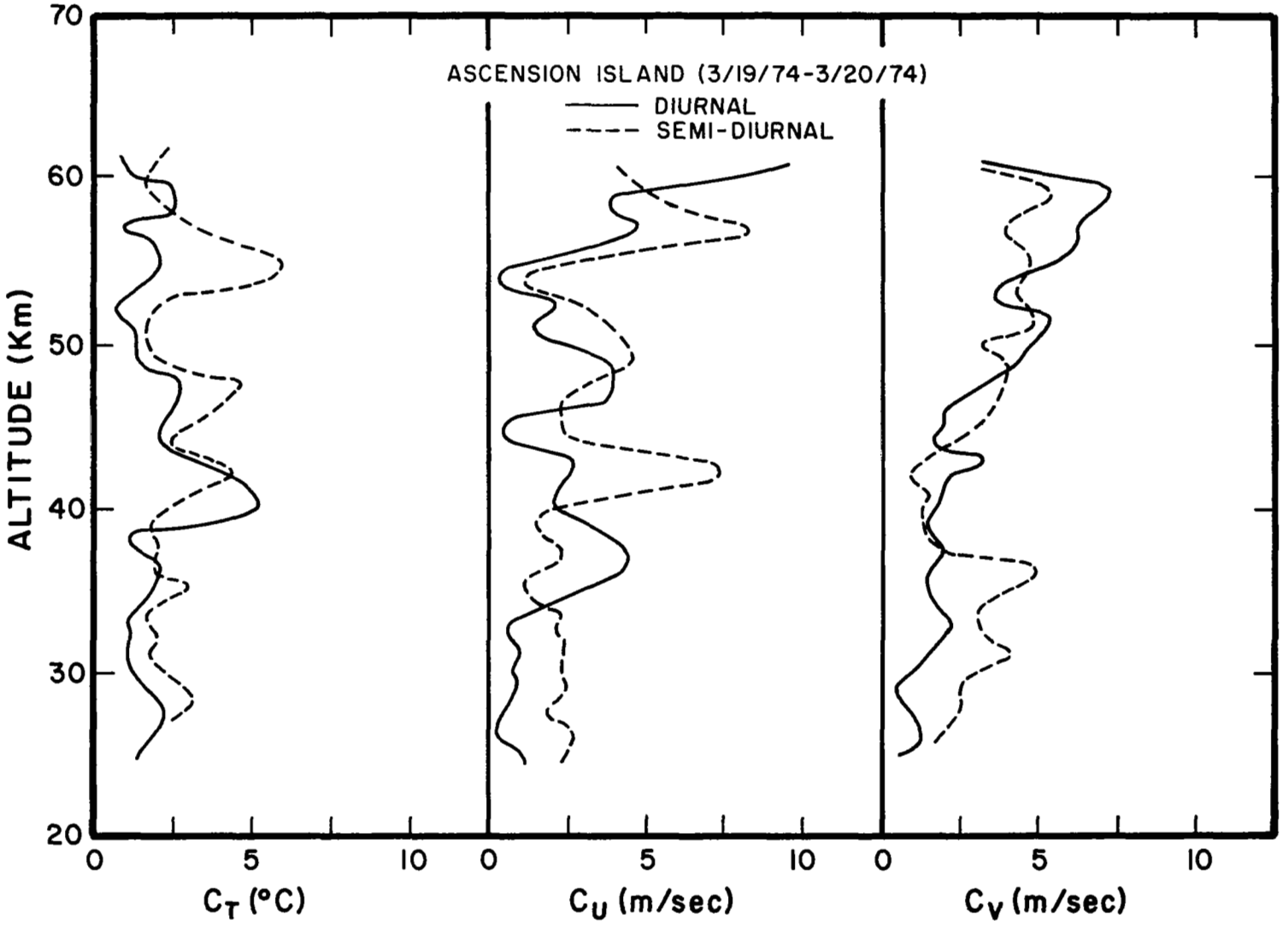


Fig. 12. Altitude distribution of the solar diurnal and semidiurnal amplitude contributions to the oscillations of temperature and zonal and meridional wind components.

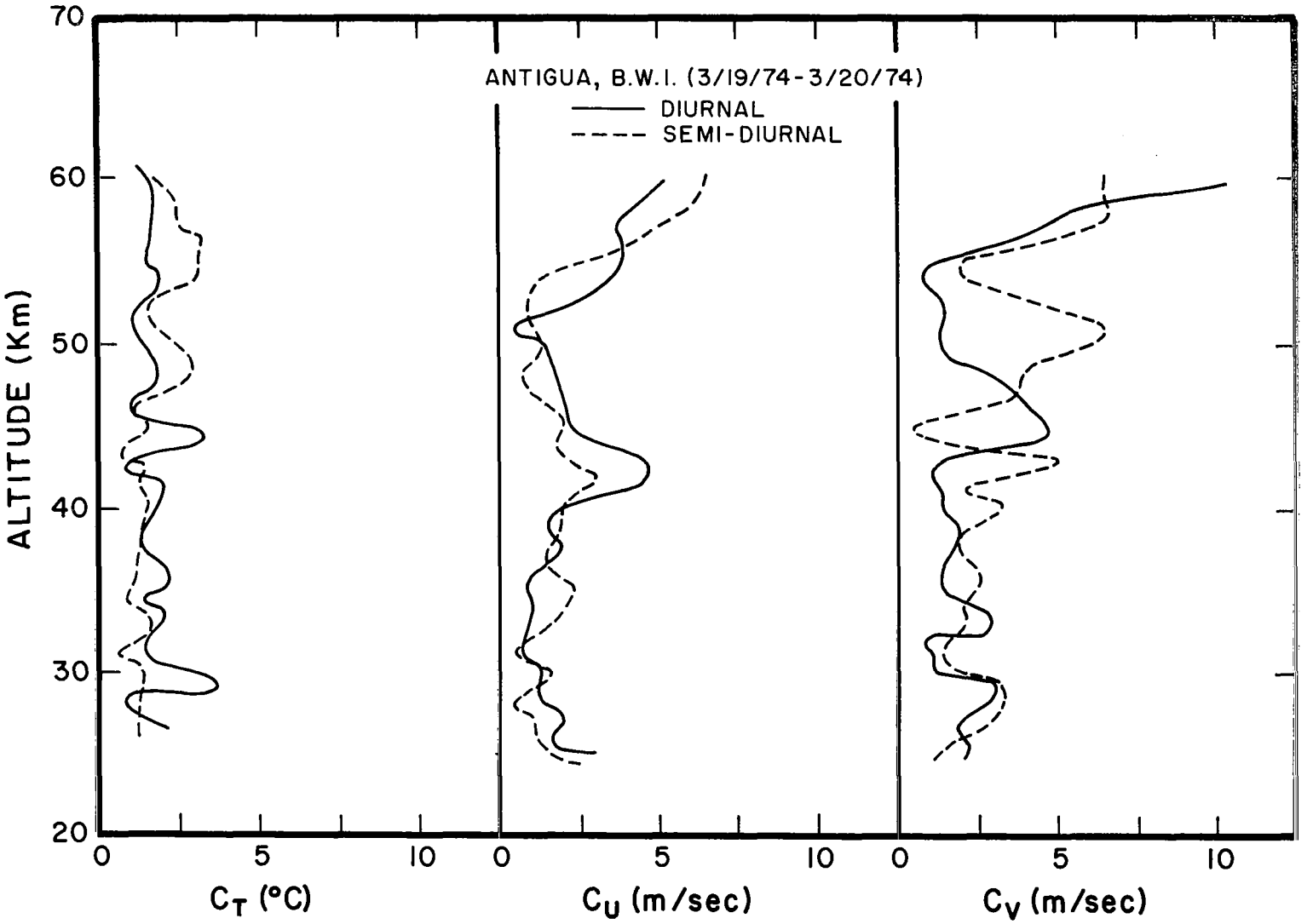


Fig. 13. Altitude distribution of the solar diurnal and semidiurnal amplitude contributions to the oscillations of temperature and zonal and meridional wind components.

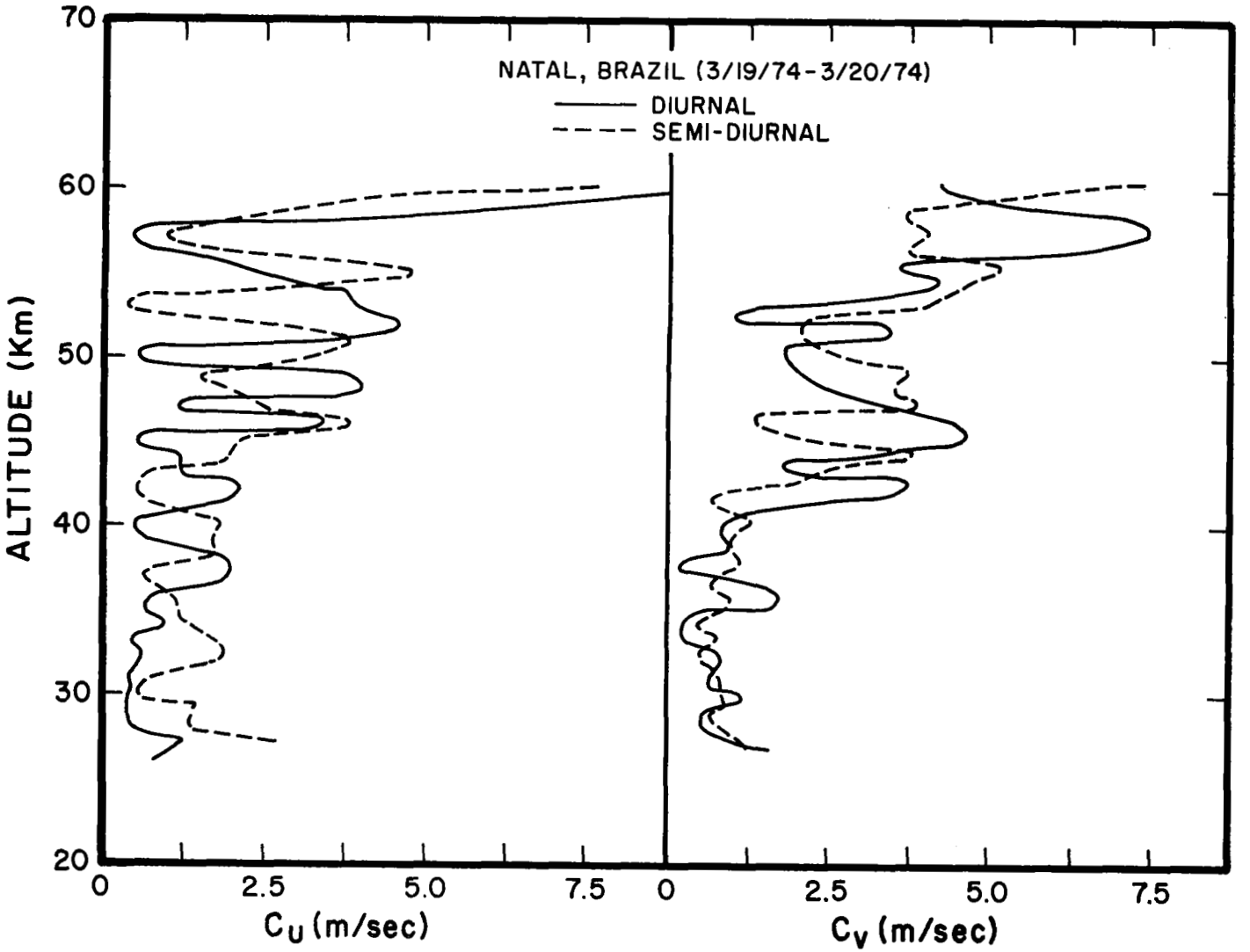


Fig. 14. Altitude distribution of the solar diurnal and semidiurnal amplitude contributions to the oscillations of the zonal and meridional wind components.

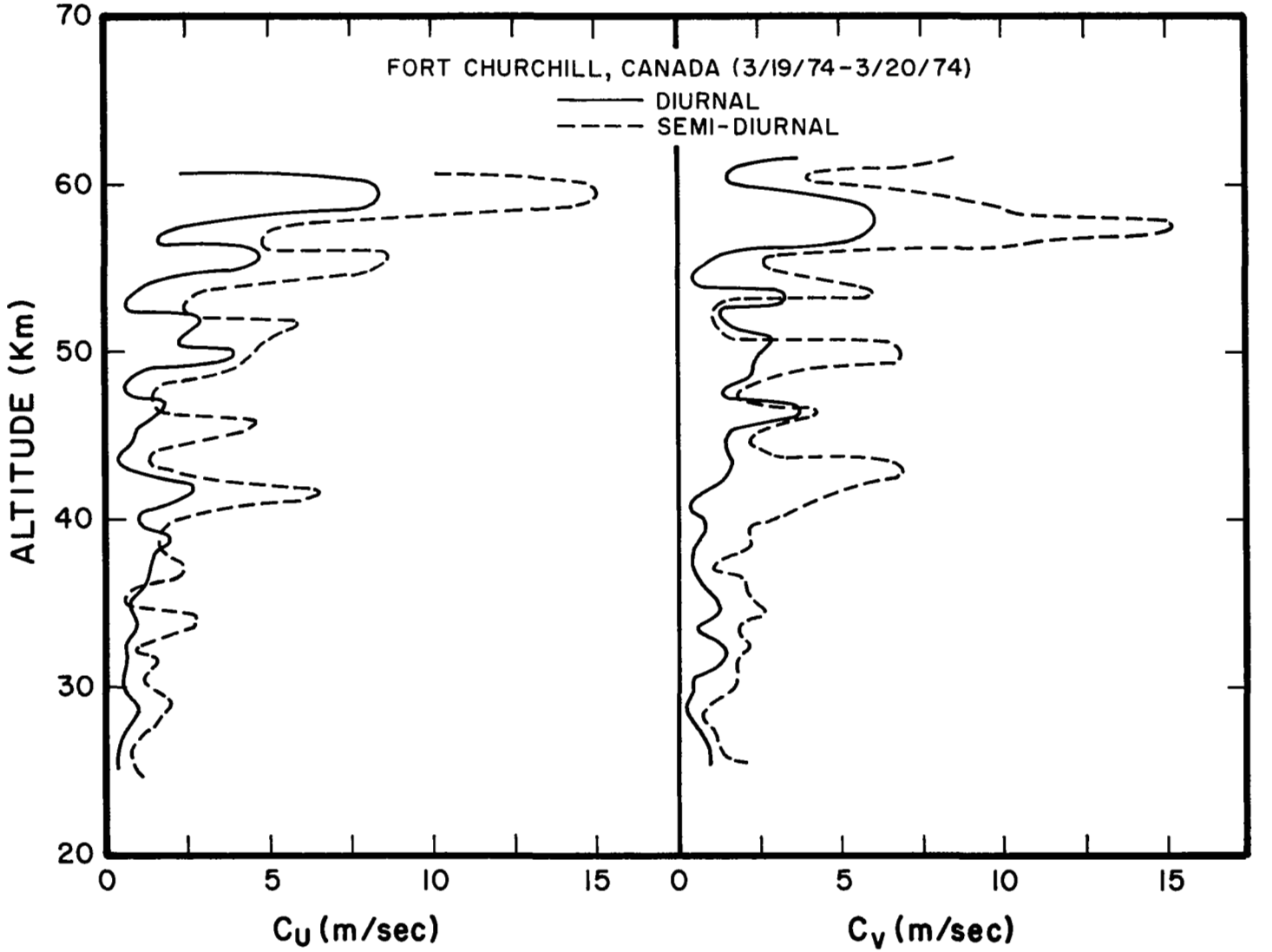


Fig. 15. Altitude distribution of the solar diurnal and semidiurnal amplitude contributions to the oscillations of the zonal and meridional wind components.

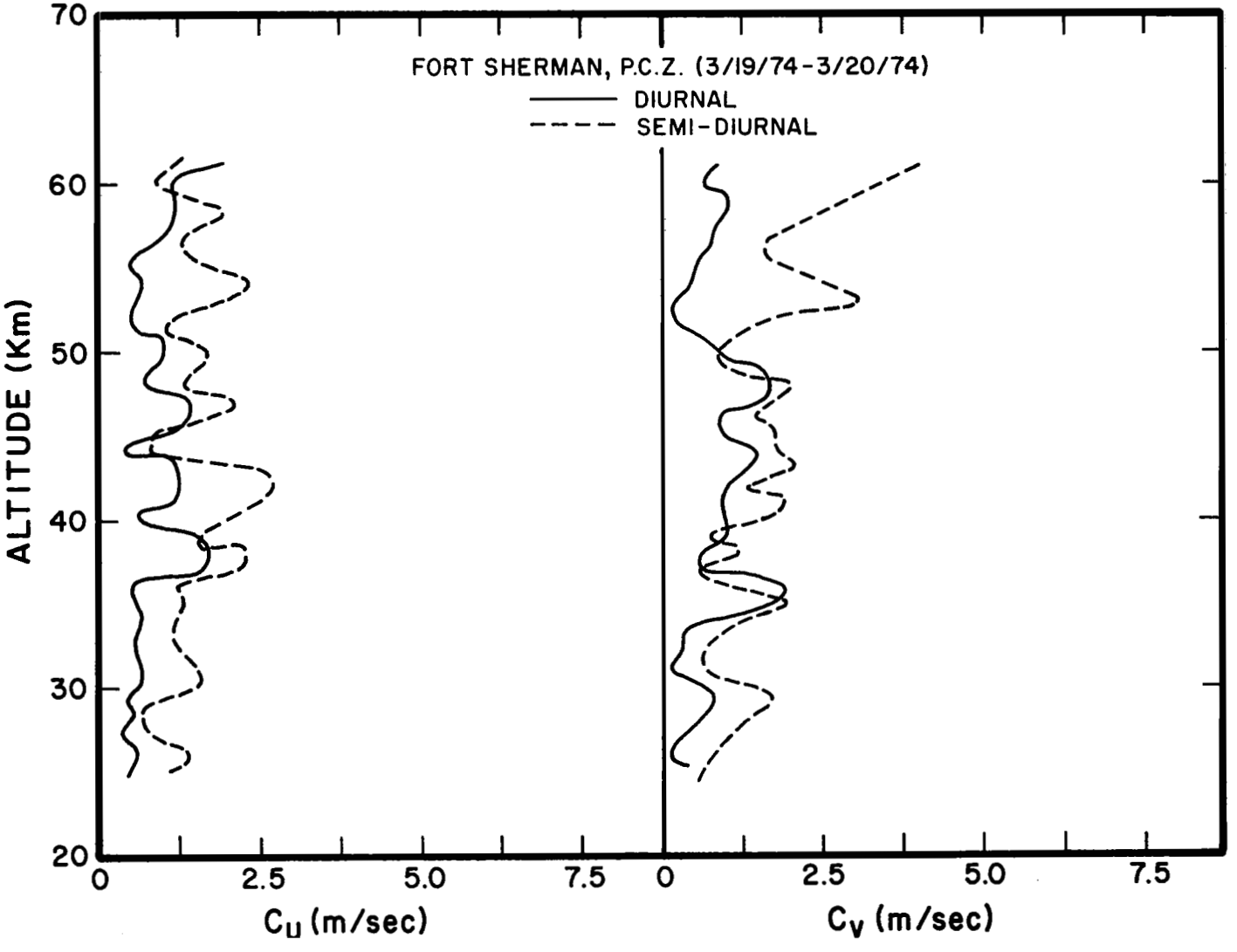


Fig. 16. Altitude distribution of the solar diurnal and semidiurnal amplitude contributions to the oscillations of the zonal and meridional wind components.

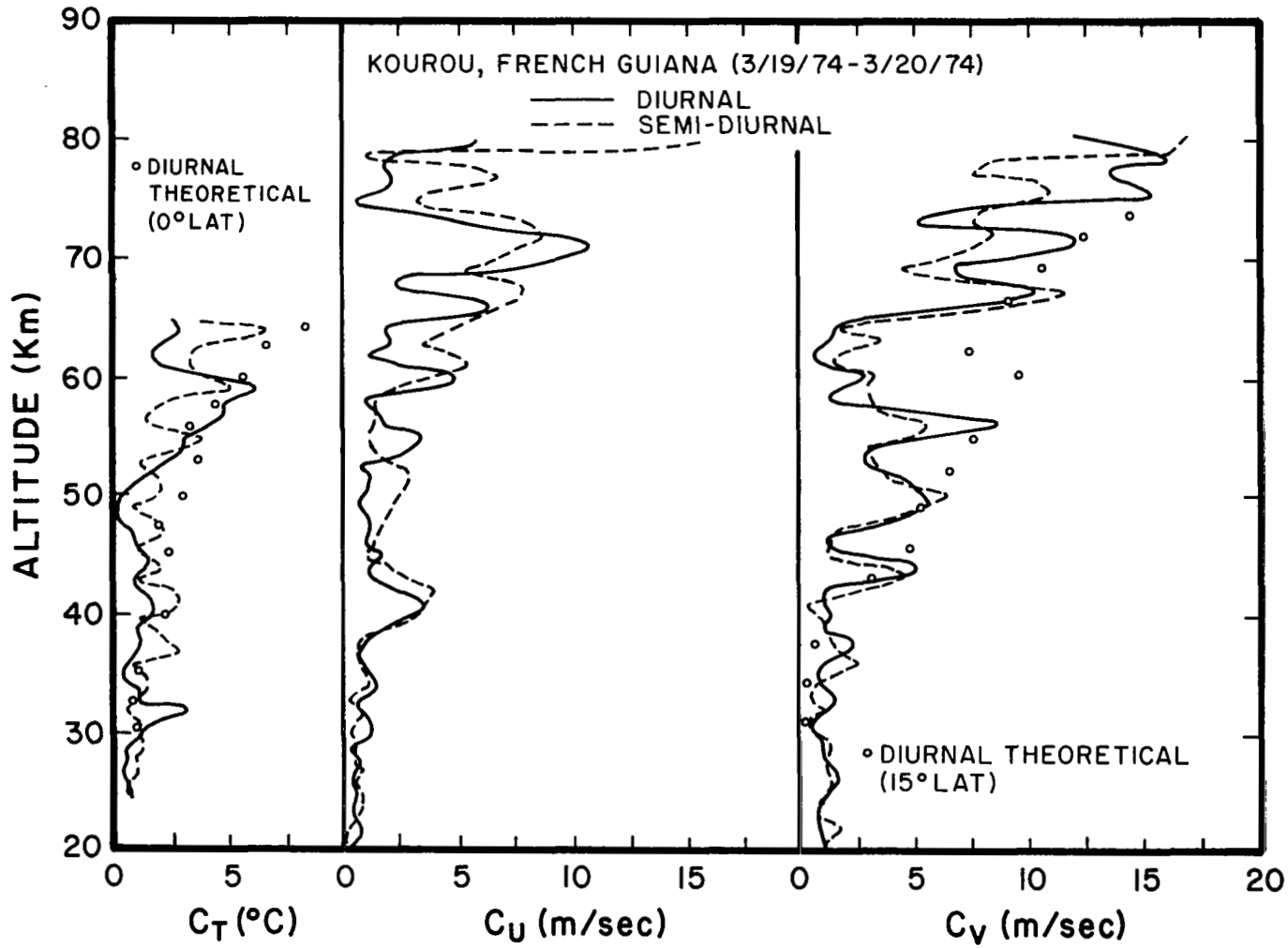


Fig. 17. Altitude distribution of the solar diurnal and semidiurnal amplitude contributions to the oscillations of temperature and zonal and meridional wind components.

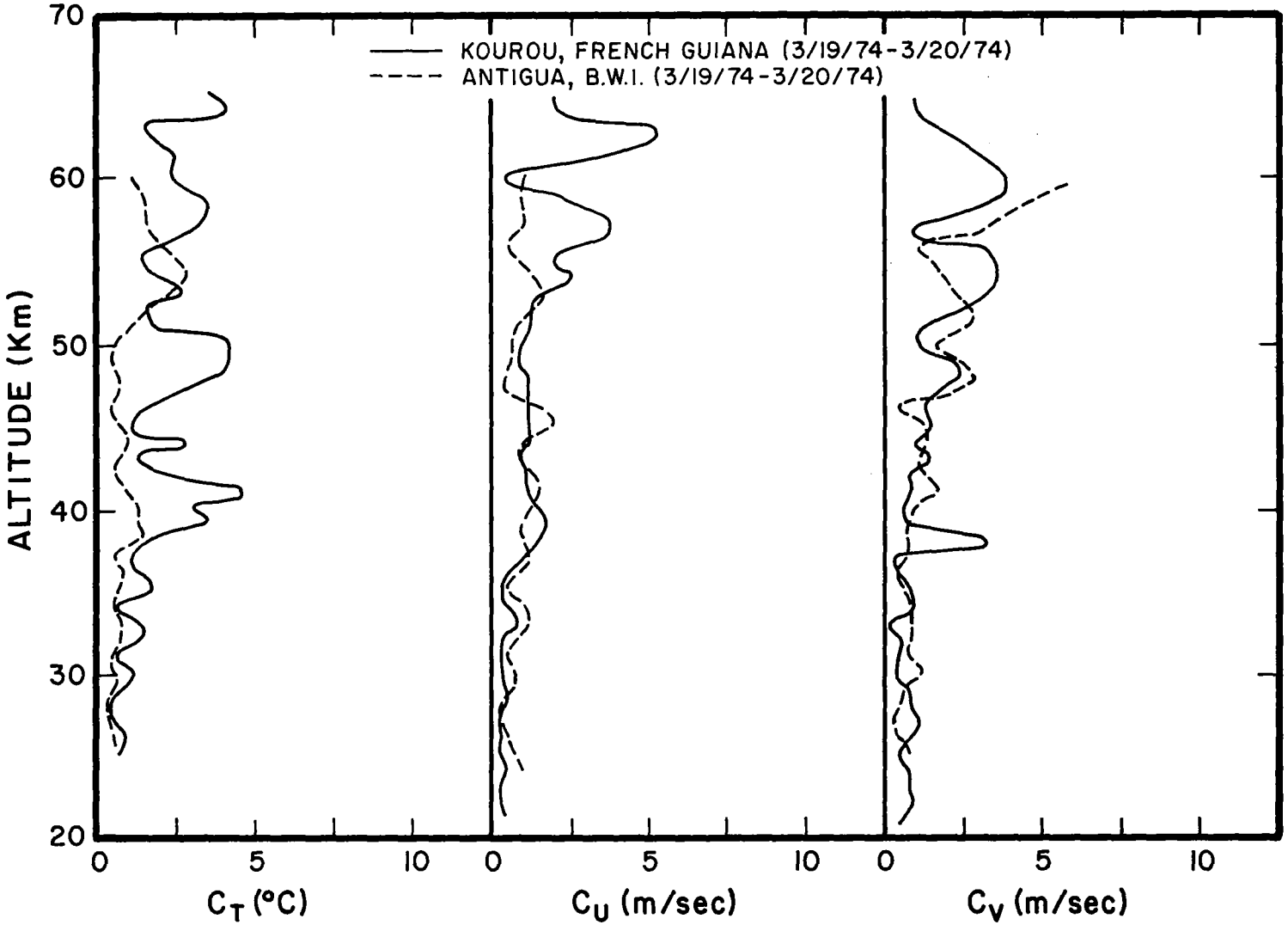


Fig. 18. Solar terdiurnal amplitude contributions to the oscillations of temperature, and zonal and meridional wind components.

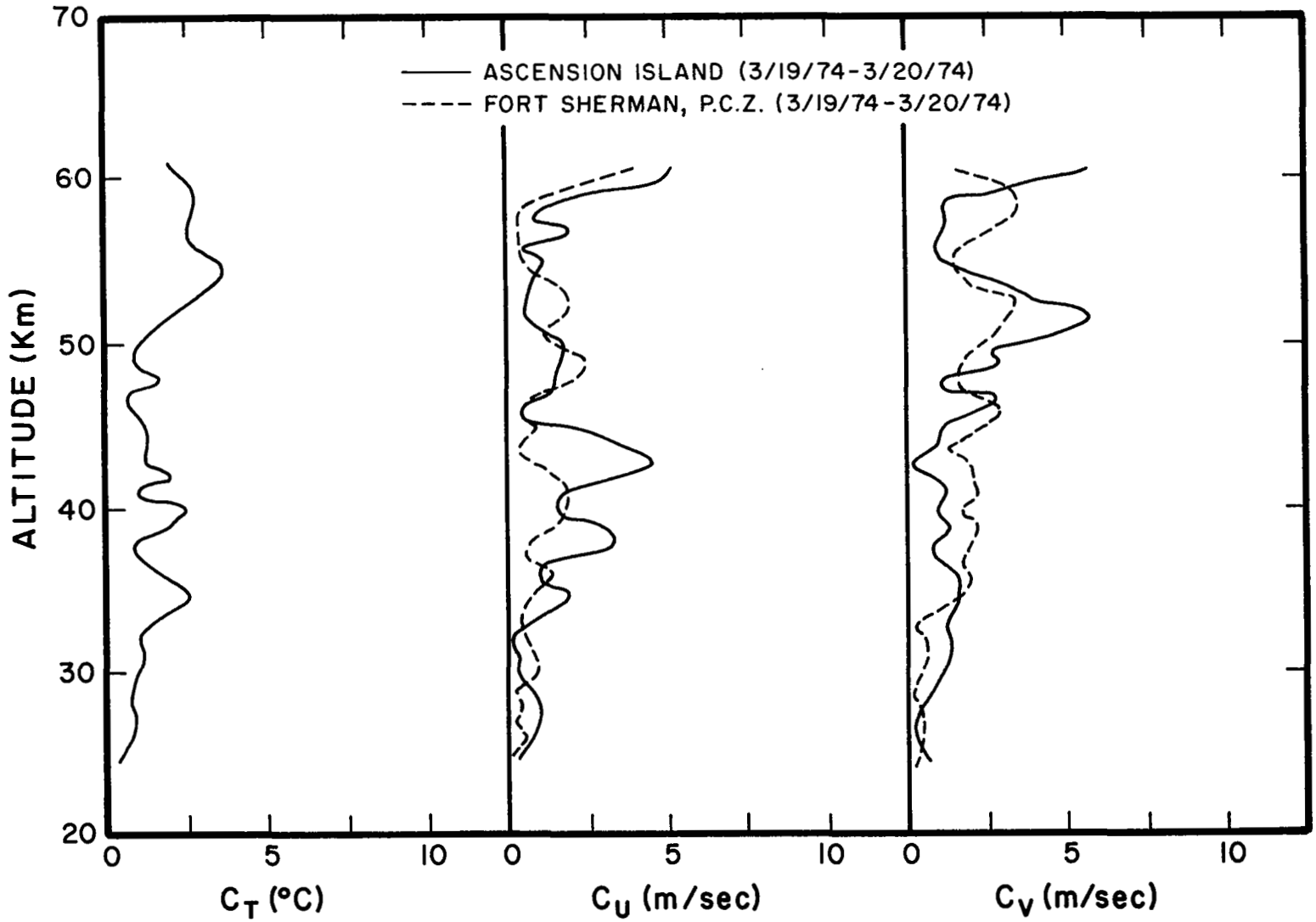


Fig. 19. Solar terdiurnal amplitude contributions to the oscillations of temperature, and zonal and meridional wind components.

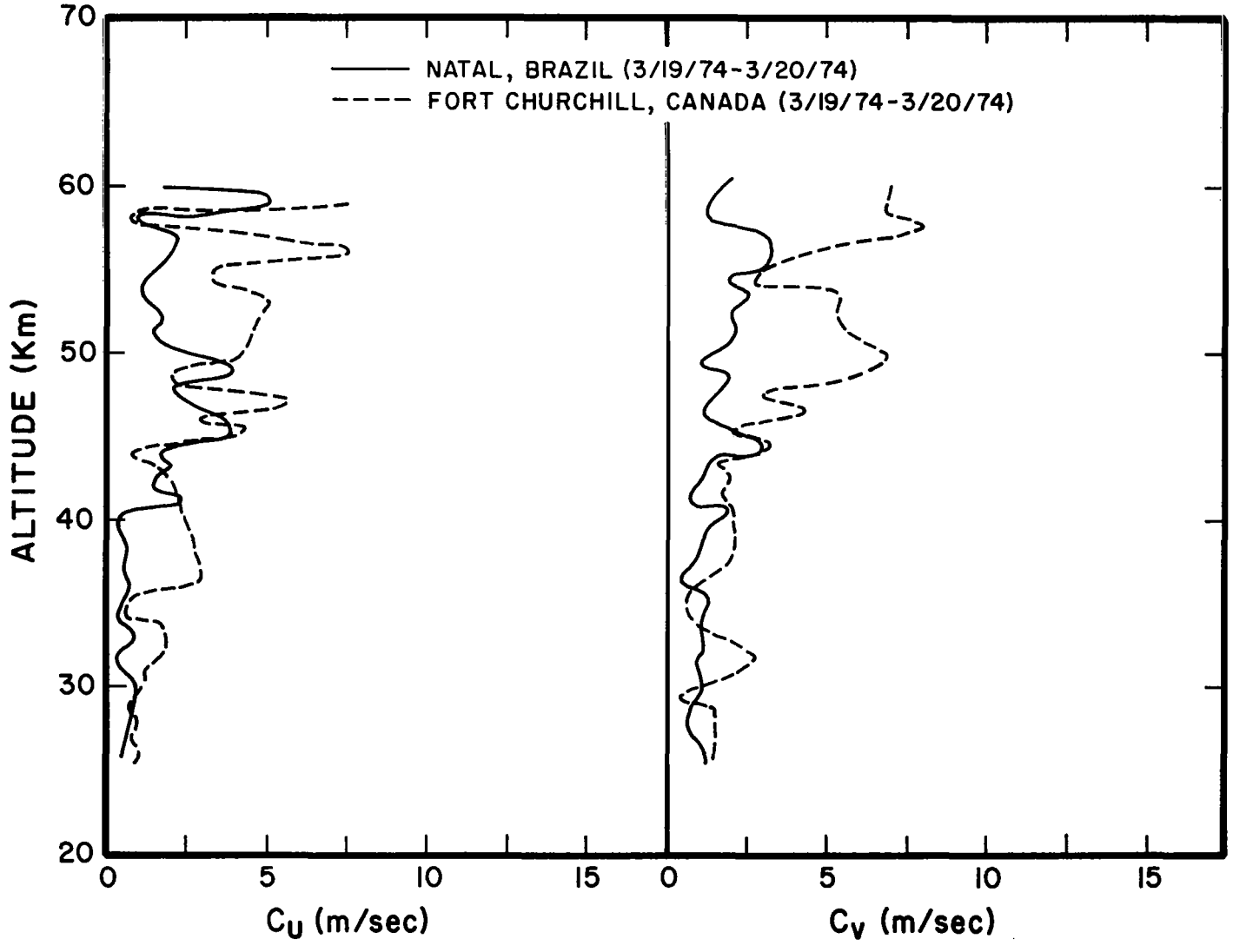


Fig. 20. Solar terdiurnal amplitude contributions to the oscillations of zonal and meridional wind components.

meridional and diurnal zonal wind oscillations respectively. Also at Fort Sherman the semidiurnal meridional wind oscillation is about 3.5 m/s while the semidiurnal zonal wind oscillation is about 1.5 m/s at 60 km.

Tidal theory (Chapman and Lindzen, 1970) predicts a diurnal amplitude of about 7 m/s at 60 km in the tropics for the meridional wind and for the semidiurnal meridional wind an amplitude of about 4 m/s. The respective amplitudes predicted by theory at 30 km for diurnal and semidiurnal meridional wind oscillations are 1 m/s and .1 m/s. Our results agree well with theoretical predictions of diurnal oscillations; however, we find a substantially higher semidiurnal meridional wind component than predicted by theory.

Figure 17 (Kourou) extends up to 80 km and shows the theoretical diurnal amplitude of the meridional wind. The agreement between observed and theoretical altitude distributions is good with the amplitude of diurnal oscillation for the meridional wind reaching about 15 m/s at 75 km. The theoretical prediction for the semidiurnal amplitude of the meridional wind is about 4 m/s at $10^{o}$ latitude and the observed is about 6 m/s.

The observed diurnal and semidiurnal temperature oscillations are between 1 and $2.5^{o}$C at 30 km and 2 and $6^{o}$C at 60 km. Figure 17 shows the theoretical altitude distribution of the diurnal temperature amplitude. The agreement is seen to be excellent.

Figures 18, 19 and 20 show terdiurnal amplitude distributions for temperature, zonal and meridional winds. In general for both meridional and zonal wind, the terdiurnal contribution is found to be about 1 m/s at 30 km in the tropics and 2.5 m/s at 60 km. At Fort Churchill ($57.1^{o}$N) the contributions to the zonal and meridional winds at 60 km are 4.5 m/s and 7 m/s respectively. Methods which presuppose only variations due to diurnal and semidiurnal oscillations break down under these circumstances, since there is a substantial terdiurnal contribution at higher altitudes.

Figures 21, 22 and 23 show the altitude distributions of phase (hour of maximum) of the solar diurnal component of the zonal wind. It is observed that for all stations except Fort Churchill there are rapid changes of phase angle with height. At Fort Churchill (Figure 22) the changes are not sharp until 51 km.

Figures 24 and 25 show the altitude distributions of phase of the solar diurnal component of the meridional wind. Figure 25 shows the theoretical phase distribution for $15^{o}$ latitude (Chapman and Lindzen, 1970). There is good agreement between observed and theoretical distributions especially for Antigua ($17.2^{o}$N); however, the observed phase angles still oscillate greatly with altitude. Since we have such a small amount of data, there is no statistical significance to our results.

Figures 26 and 27 show the altitude distributions of phase of the solar semidiurnal component of the zonal wind. A rapid phase angle shift of about $180^{o}$ is seen at Ascension (Figure 26) at 35 km.

Figures 28 and 29 show the altitude distributions of phase of the solar semidiurnal component of the meridional wind. Figure 28 shows the theoretical distribution for $10^{o}$ latitude. The agreement between theoretical and observed phase distributions is best for Ascension Island ($8.0^{o}$S). As is evident from Figures 26, 27, 28 and 29, the phase variations with height are also rapid for the semidiurnal component of the zonal and meridional winds, but only at Ascension Island for the zonal wind at 35 km is the phase change about $180^{o}$.

Figure 30 shows the altitude distribution of phase of the solar terdiurnal component of the zonal wind for Ascension Island and Kourou. Little theoretical work has been done on this oscillation. The phase change with height is more gradual than for diurnal or semidiurnal oscillations.

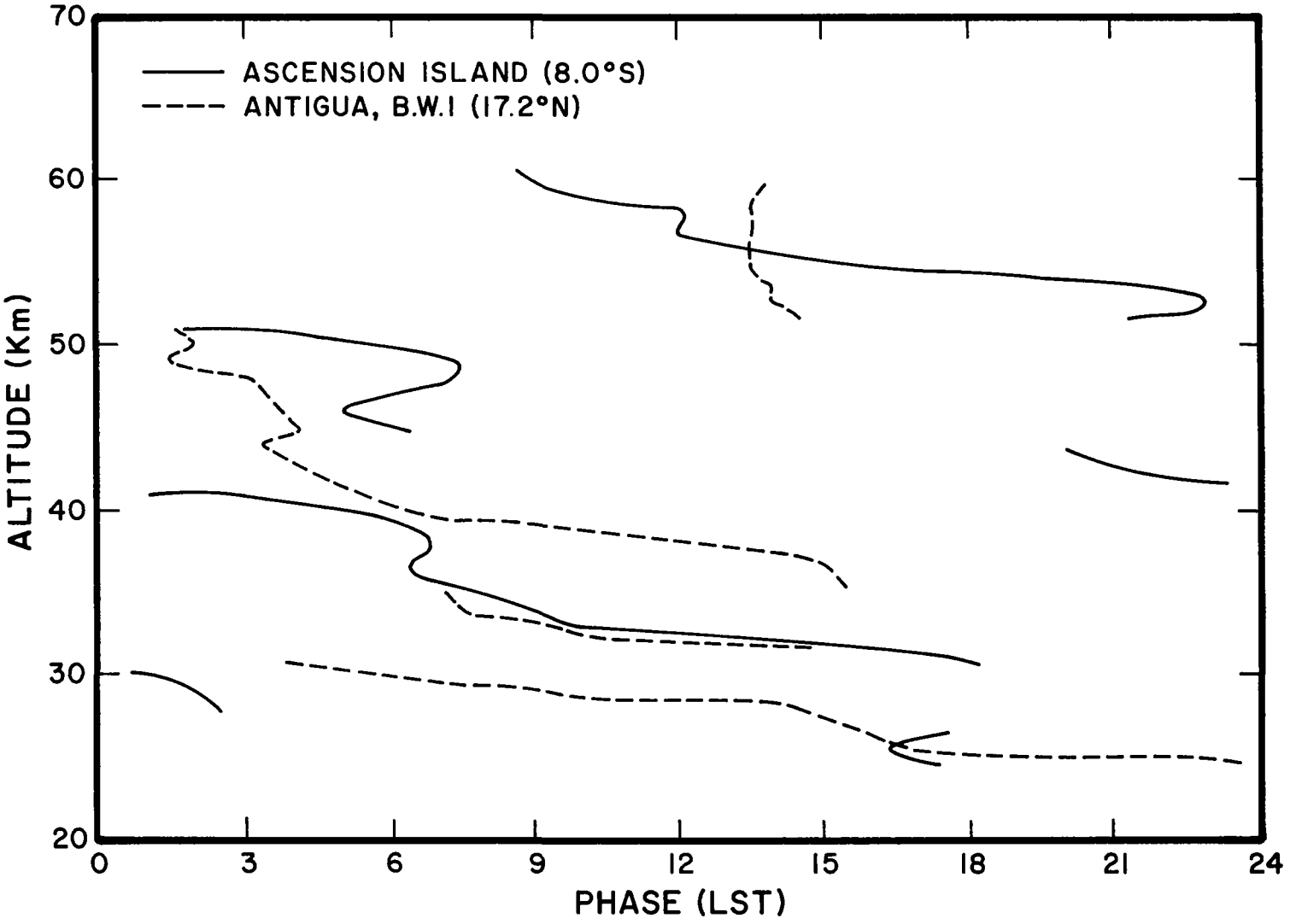


Fig. 21. Altitude distributions of phase (hour of maximum) of the solar diurnal component of zonal wind for 19-20 March 1974.

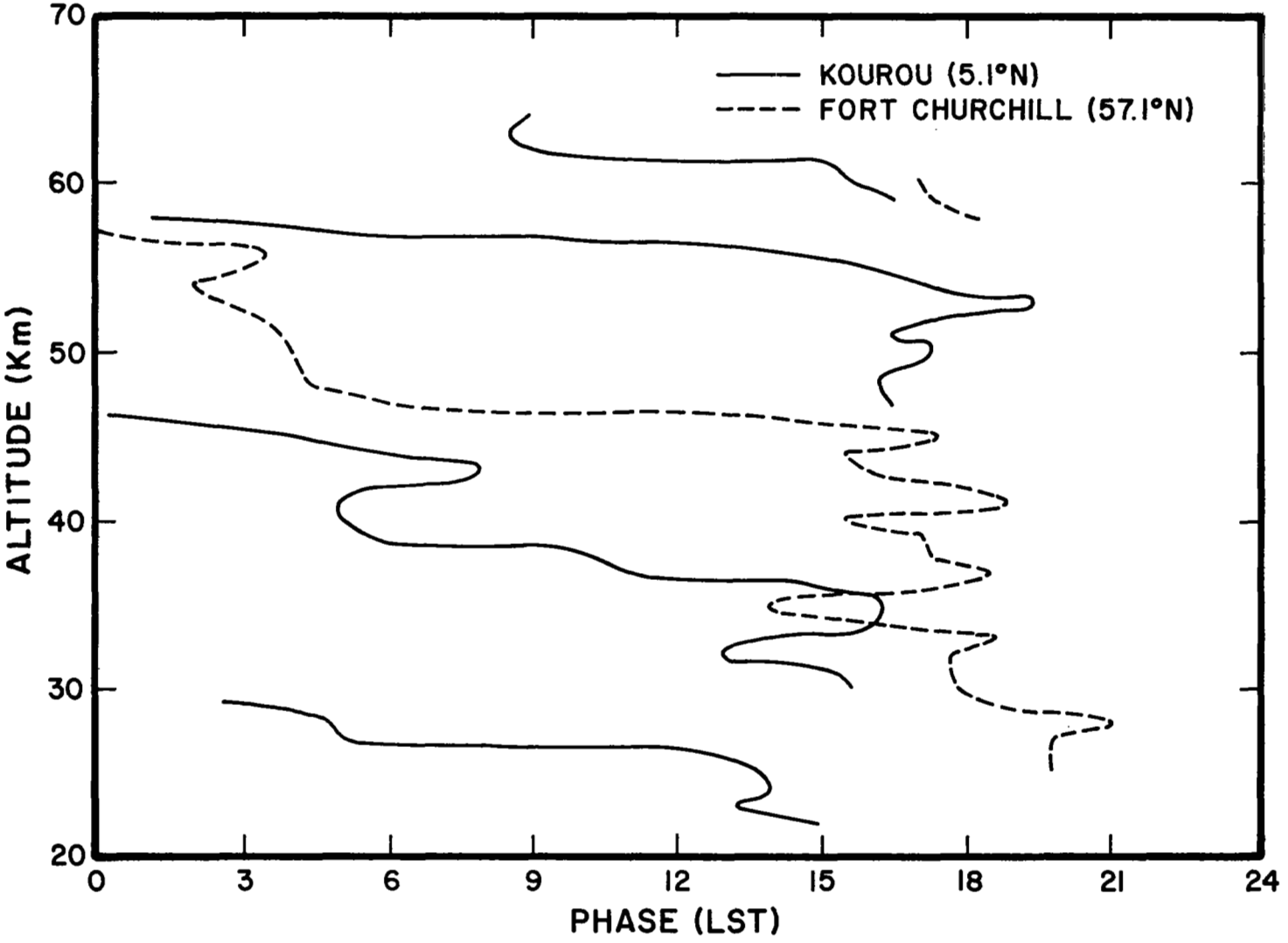


Fig. 22. Altitude distributions of phase (hour of maximum) of the solar diurnal component of zonal wind for 19-20 March 1974.

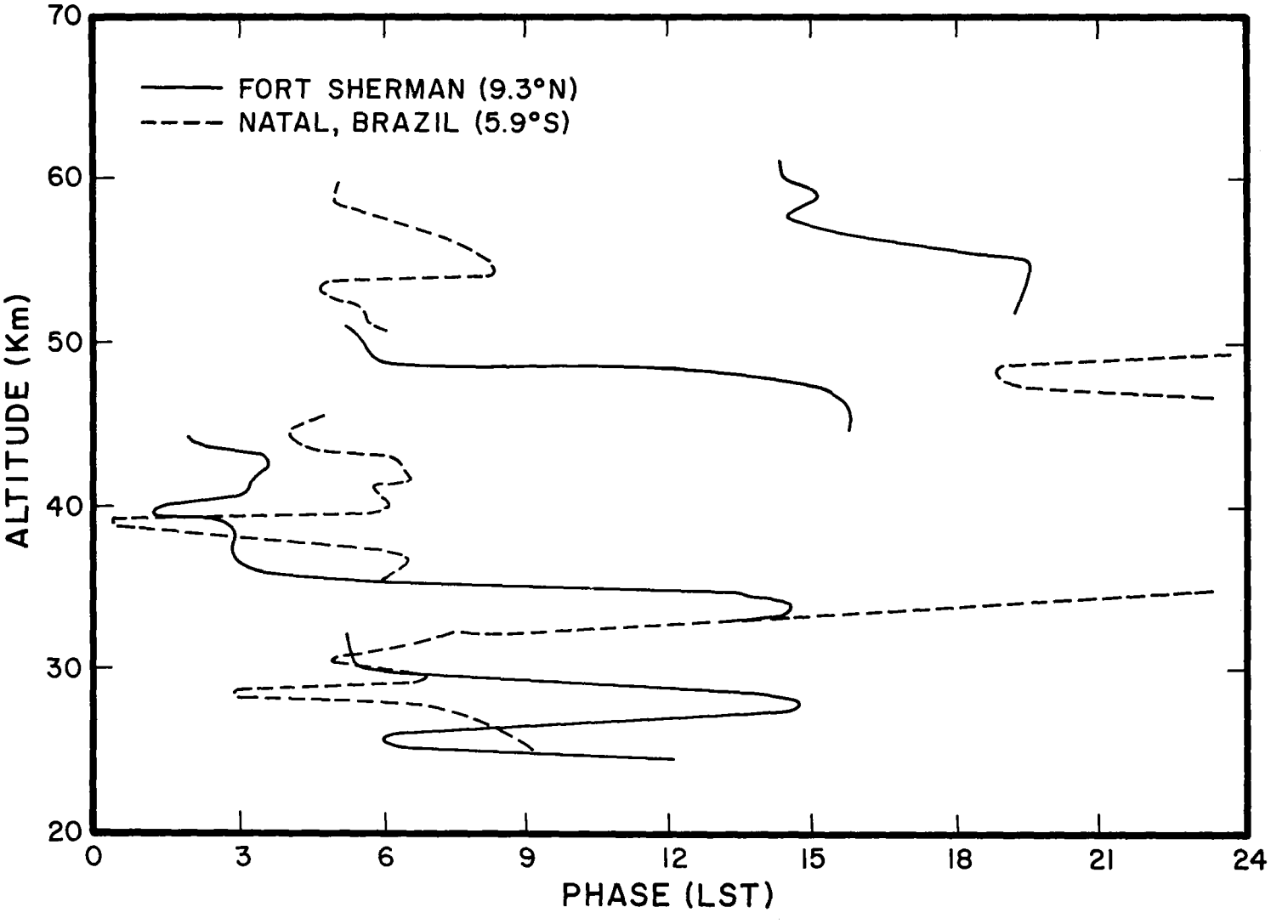


Fig. 23. Altitude distributions of phase (hour of maximum) of the solar diurnal component of zonal wind for 19-20 March 1974.

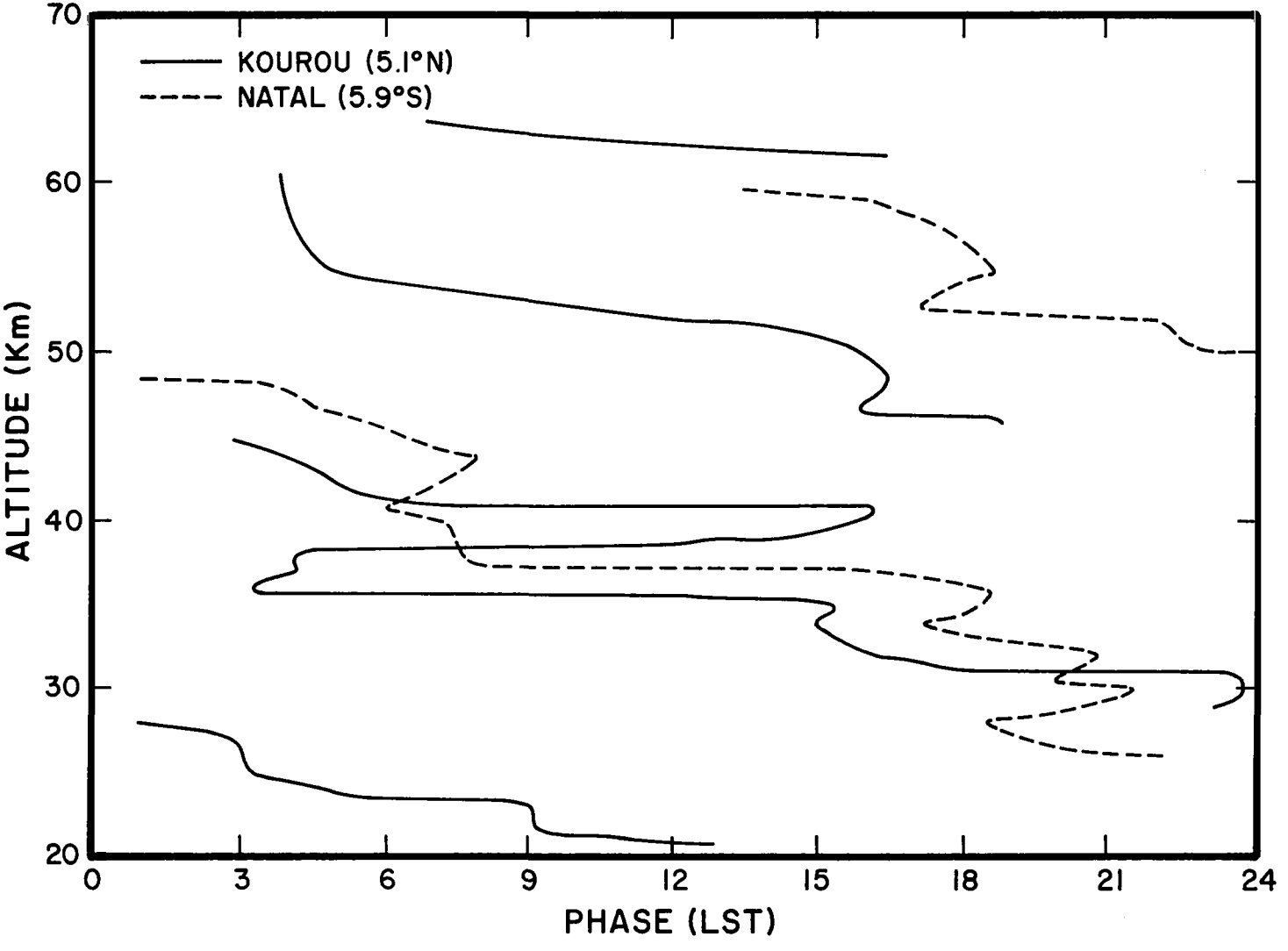


Figure 24. Altitude distributions of phase (hour of maximum) of the solar diurnal component of meridional wind for 19-20 March 1974.

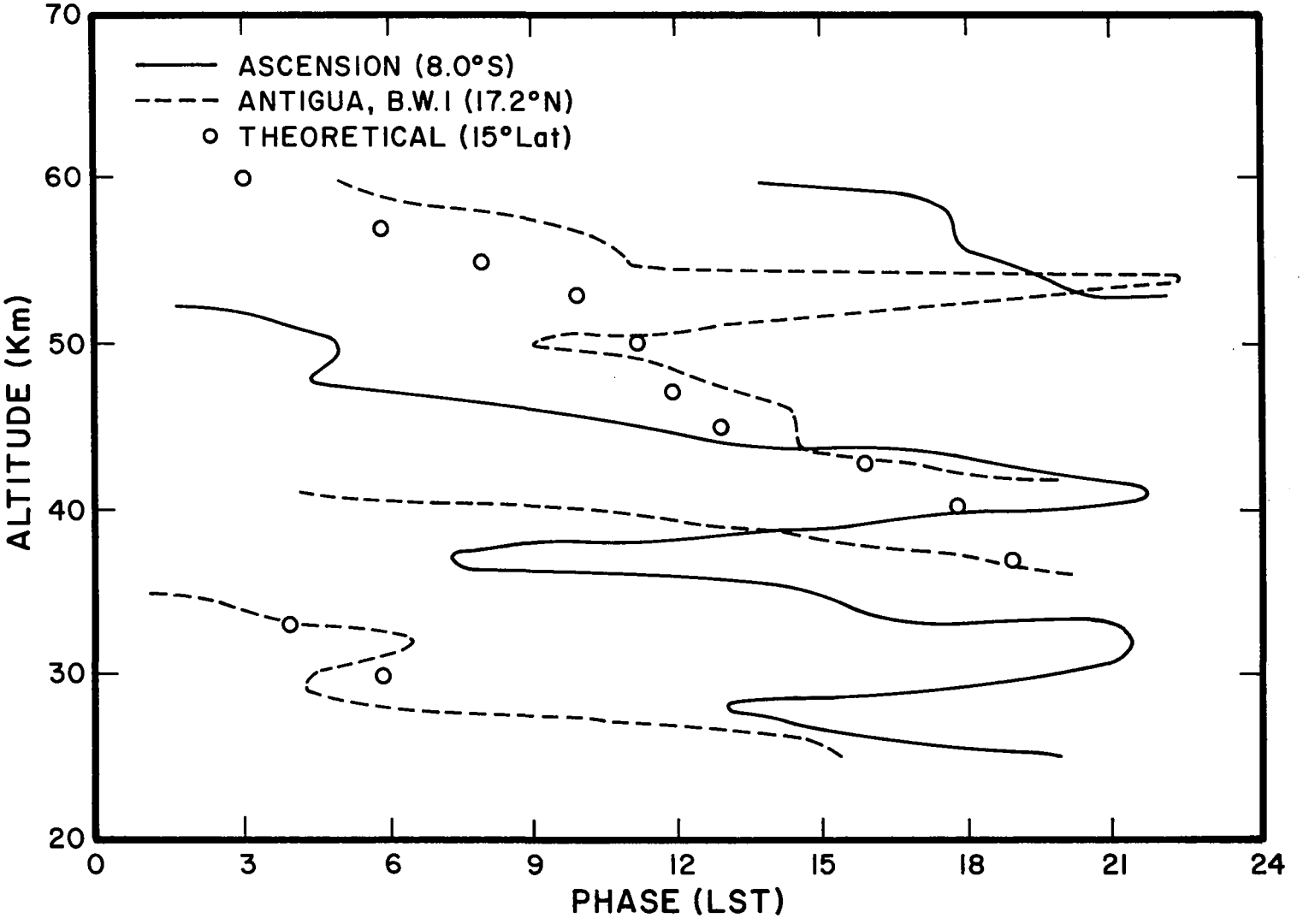


Fig. 25. Altitude distributions of phase (hour of maximum) of the solar diurnal component of meridional wind for 19-20 March 1974.

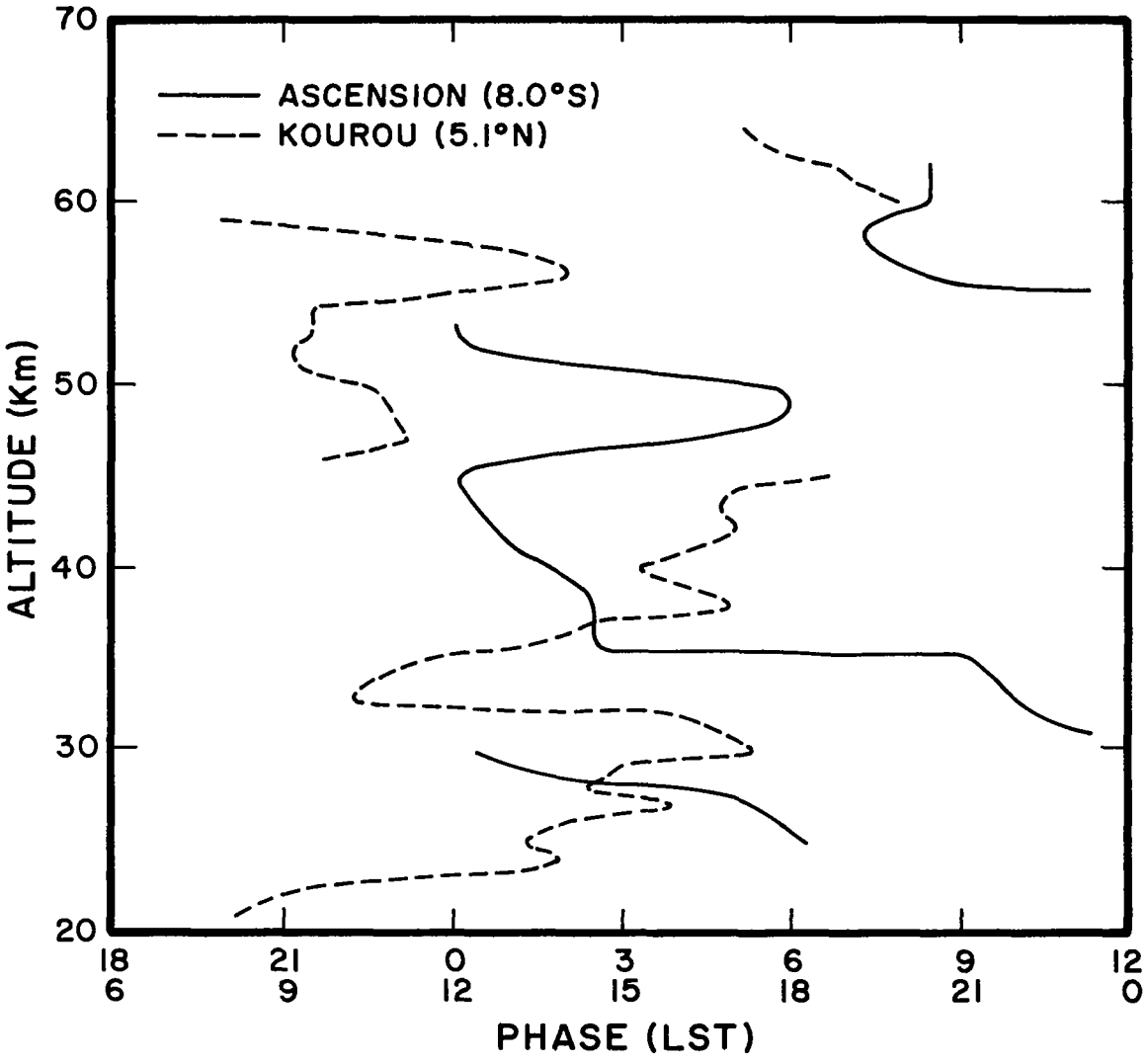


Fig. 26. Altitude distributions of phase (hour of maximum) of the solar semidiurnal component of the zonal wind for 19-20 March 1974.

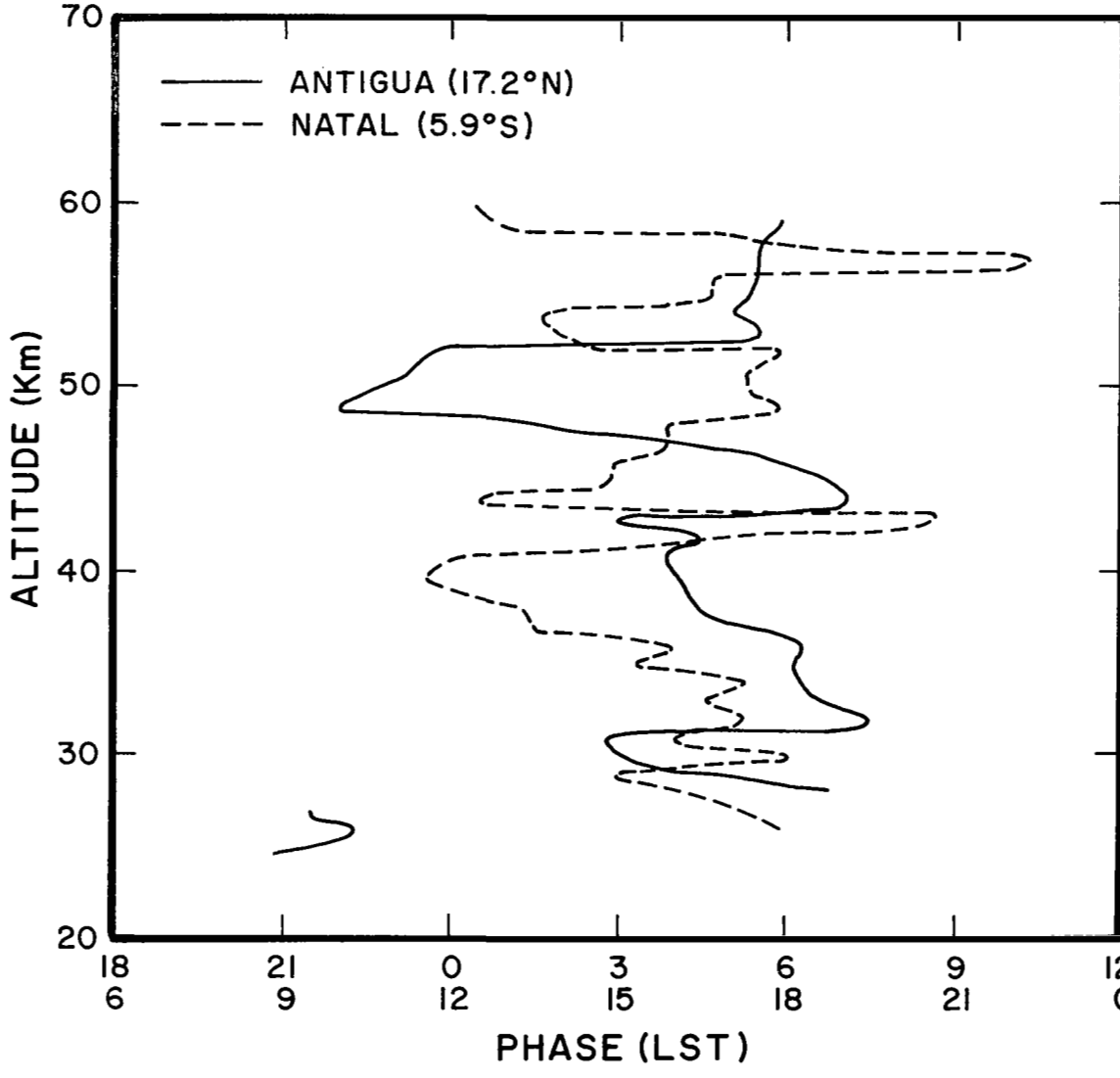


Fig. 27. Altitude distributions of phase (hour of maximum) of the solar semidiurnal component of the zonal wind for 19-20 March 1974.

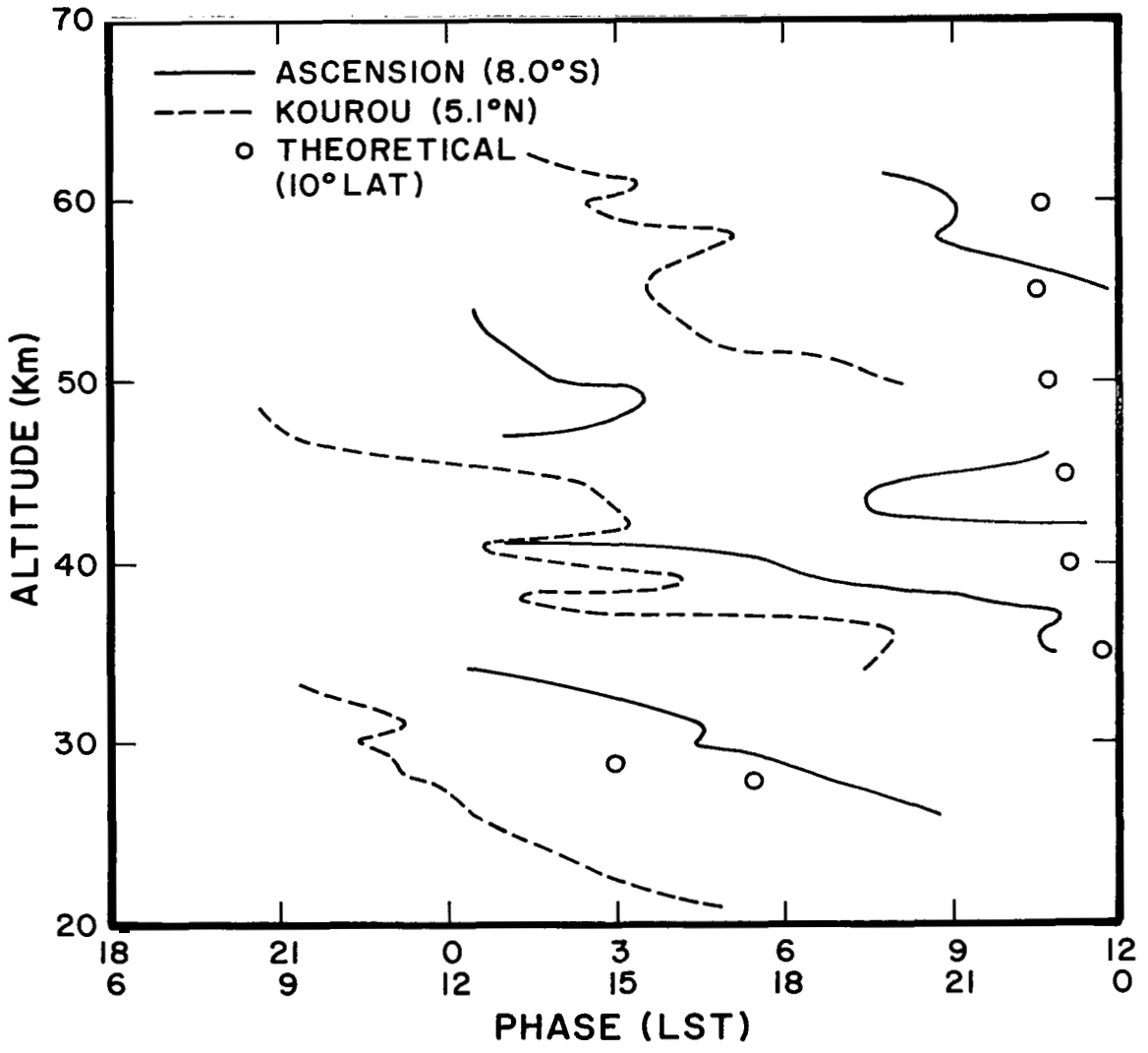


Fig. 28. Altitude distributions of phase (hour of maximum) of the solar semidiurnal component of the meridional wind for 19-20 March 1974.

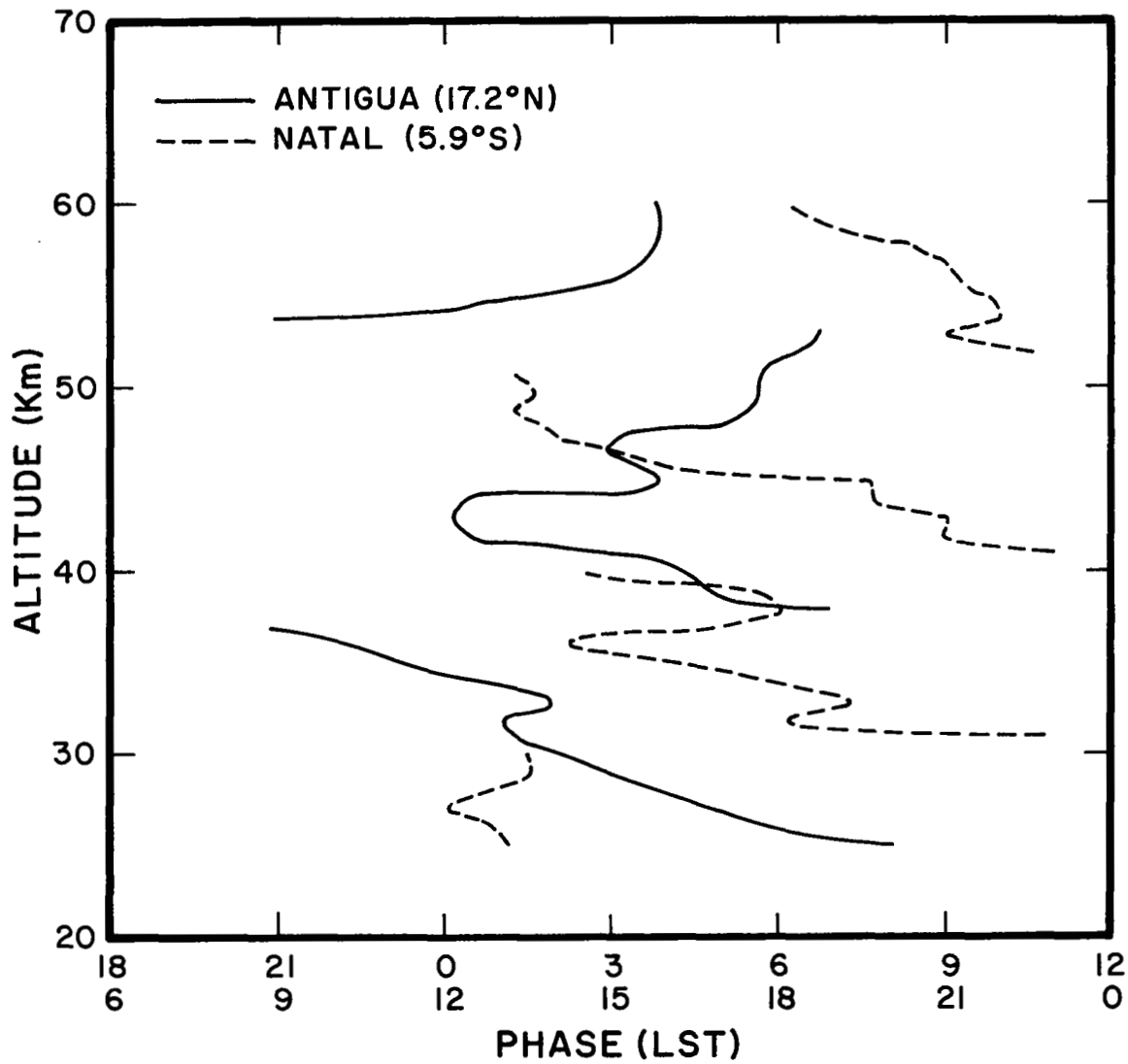


Fig. 29. Altitude distributions of phase (hour of maximum) of the solar semidiurnal component of the meridional wind for 19-20 March 1974.

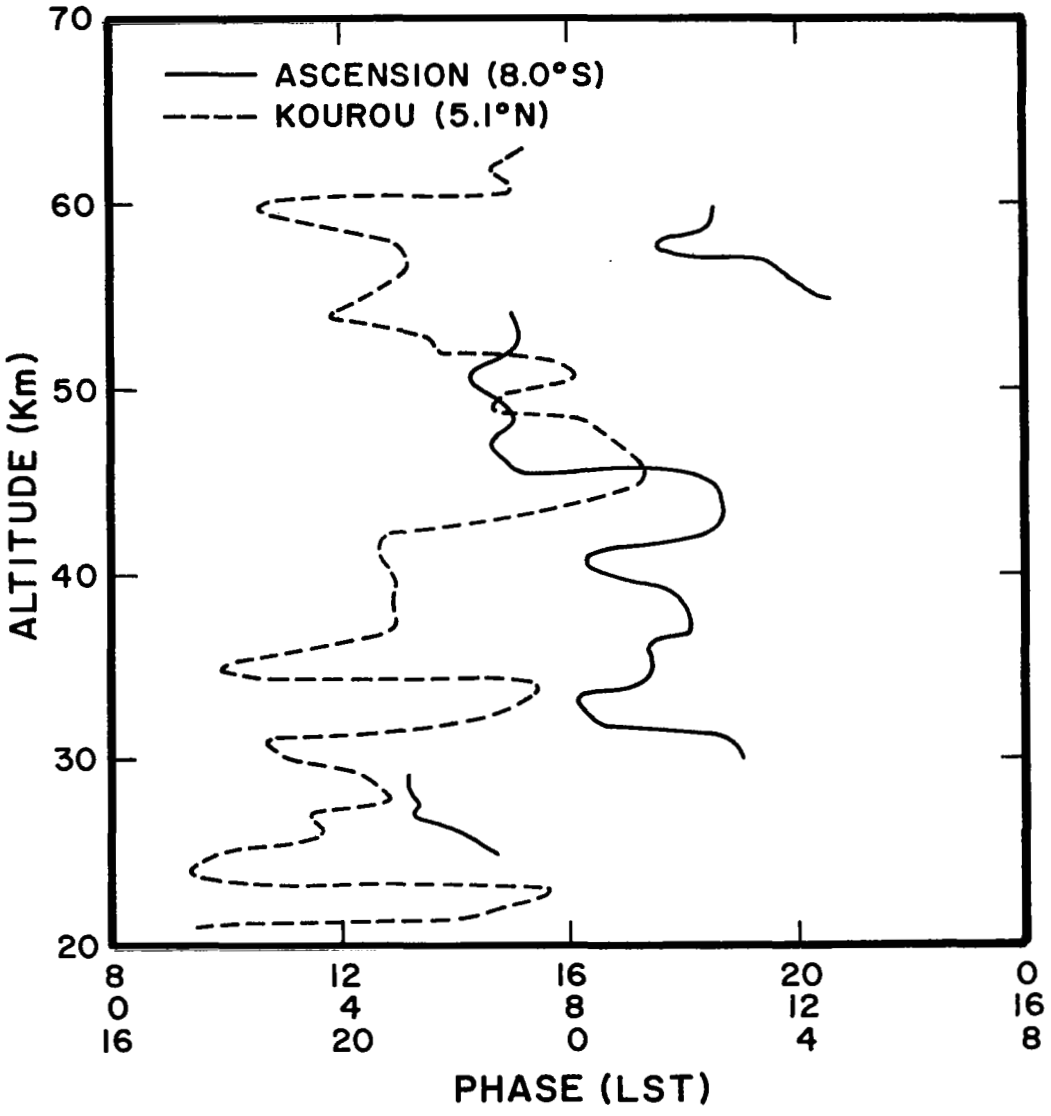


Fig. 30. Altitude distributions of phase (hour of maximum) of the solar terdiurnal component of the zonal wind for 19-20 March 1974.

## SUMMARY AND CONCLUSIONS

Analysis of the meteorological rocket data obtained from an experiment conducted at 3-hour intervals on 19-20 March 1974 at 8 western meridional rocket stations indicate that:

1) Large variations in the meridional wind contribute substantially to overall turbulence in the tropical stratosphere.

2) The solar semidiurnal component of wind oscillations in the tropics was observed to be much higher than predicted by theory, often exceeding the magnitude of the diurnal amplitude throughout the stratosphere.

3) The observed value of the solar diurnal amplitude in the stratosphere was in line with theoretical predictions.

4) The solar terdiurnal amplitudes for temperature, meridional and zonal winds were non-negligible and must be considered in any harmonic analysis.

5) Phase angle variation with height was rapid for all harmonics; however, there was general agreement between predicted and observed phase angles.

6) Because of large changes in the mean winds in the mesosphere with season, harmonic determinations are difficult. There appear to be large zonal wind changes even within the same season as mentioned previously.

7) Turbulence diffusivity in the upper stratosphere is greater near the equator than in the mid-latitudes.

Much more data is needed before statistically significant determination of harmonic amplitudes and phase angles can be made. Little work has been done on the variation of these amplitudes and phase angles with season.

Other areas which must be explored before a true picture of the dynamic structure of the stratosphere and mesosphere is obtained are contributions of nonlinear terms in the governing equations and the possible cascade of tidal energy downward in scale to higher frequencies. In order to ascertain the structure of turbulence in the stratosphere and mesosphere

a full nonlinear treatment would seem necessary. Kousky and Koermer (1974) have recently shown that nonlinearity of Kelvin waves leads to turbulent dissipation in the stratosphere.

ACKNOWLEDGEMENTS

The authors wish to thank F. J. Schmidlin for his many valuable discussions and assistance. This research is sponsored by the National Aeronautics and Space Administration, Contract NAS 6-2498.

## REFERENCES


Beyers, N. J.; Miers, B. T.; and Reed, R. J.: Diurnal Tidal Motions near the Stratopause during 48 Hours at White Sands Missile Range. J. Atmos. Sci., 23, 325-333, 1966.

Booker, J. R.; and Bretherton, F. P.: The Critical Layer for Internal Gravity Waves in a Shear Flow. J. Fluid Mech., 27, 513-539, 1967.

Chapman, S.; and Lindzen, R. S.: Atmospheric Tides. Dordrecht, Holland, Reidel, pp 200, 1970.

Conte, S. D.; and deBoor, C.: Elementary Numerical Analysis. New York, McGraw-Hill, 233-241, 1972.

Kao, S.-K.; and Sands, E. E.: Energy Spectrums, Mean and Eddy Kinetic Energies of the Atmosphere between Surface and 50 Kilometers. J. Geophys. Res., 71, 5213-5219, 1966.

Kousky, V. E.; and Koermer, J. P.: The Nonlinear Behavior of Atmospheric Kelvin Waves. J. Atmos. Sci., 31, 1777-1783, 1974.

Lindzen, R. S.: The Application and Applicability of Terrestrial Atmospheric Tidal Theory to Venus and Mars. J. Atmos. Sci., 27, 536-549, 1970.

Lindzen, R. W.; and Hong, S.-S.: Effects of Mean Winds and Horizontal Temperature Gradients on Solar and Lunar Semidiurnal Tides in the Atmosphere. J. Atmos. Sci., 31, 1421-1446, 1974.

Panofsky, H. A.; and Brier, G.: Some Applications of Statistics to Meteorology. Mineral Industries Continuing Education, University Park, Pennsylvania State University, 126-138, 1965.

Reed, R. J.: Semidiurnal Tidal Motions between 30 and 60 km. J. Atmos. Sci., 24, 315-317, 1967.

Reed, R. J.; McKenzie, D. J.; and Vyverberg, J. C.: Diurnal Tidal Motions between 30 and 60 km in Summer. J. Atmos. Sci., 23, 416-423, 1966.

Reed, R. J.; Oard, M. J.; and Sieminski, M: A Comparison of Observed and Theoretical Diurnal Tidal Motions between 30 and 60 km. Mon. Wea. Rev., 97, 456-459, 1969.